Facile synthesis and anion binding properties of a preorganized macrocyclic receptor

Channi Cheng, Zhengxiang Li, Dezhi Zhao and Chengyou Han*

Department of Chemistry, College of Chemistry and Chemical Engineering, China University of Petroleum (East China), Qingdao, 266580, P. R. China

E-mail: hanchengyou@upc.edu.cn

Supporting Information (29 pages)

1. *Materials and methods*

All reagents were commercially available and purchased from Adamas-beta® reagent company which were used as supplied without further purification. Solvents were either employed as purchased or dried according to methods described in the literature. All NMR spectra were obtained on a Bruker Ascend™ 400 MHz spectrometer. The melting points were acquired on an SGW®X-4A micro melting point apparatus. High-resolution mass spectrometry (HRMS) measurements were performed on a G2-XS QTof. Ultraviolet-visible (UV-vis) spectra were collected spectra on a Shimadzu UV2550.

2. *Synthetic routes for **MR***

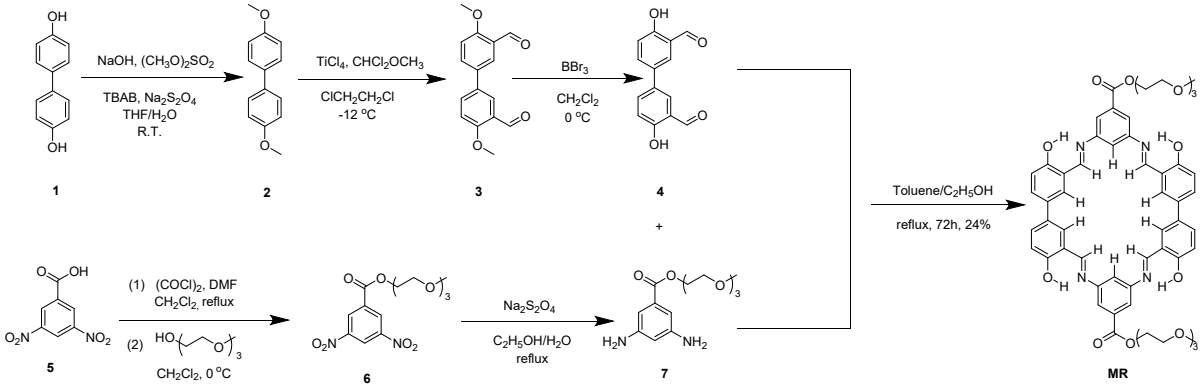

Scheme S1. Synthesis of **MR**.

3. *Synthesis of **2**[S1]*

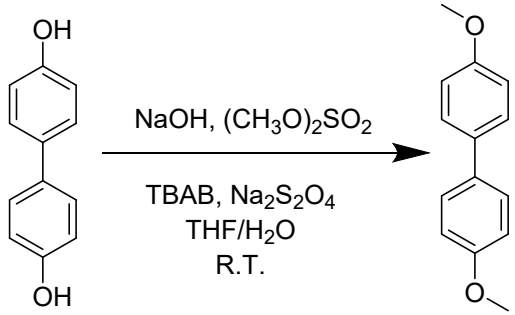

1 **2**

In a 250 mL round–bottom flask, 4,4'-biphenol **1** (10.0 g, 53.7 mmol) in a mixture of THF (120 ml) and H_2O (60 ml) was dissolved, and then tetrabutylammonium bromide (TBAB) (1.40 g, 4.30 mmol), sodium dithionite (0.75 g, 4.30 mmol) and

NaOH (10.0 g, 250 mmol) were added. The reaction mixture was stirred at room temperature for 15 min, and dimethyl sulfate (22.0 ml, 232 mmol) was added slowly for 10 minutes. The reaction mixture was stirred continuously at room temperature for 2 h. The resulting solid was collected by filtration to give **2** as a white solid (11.50 g, 100%), M.p.179.2–181.5 °C.^{1}H NMR (400 MHz, $CDCl_3$, room temperature) δ (ppm): 7.48 (d, J = 8.9 Hz, 4H), 6.96 (d, J = 8.9 Hz, 4H), 3.84 (s, 6H). ^{13}C NMR (100 MHz, $CDCl_3$, room temperature) δ (ppm):158.69, 133.50, 127.75, 114.17, 55.37.

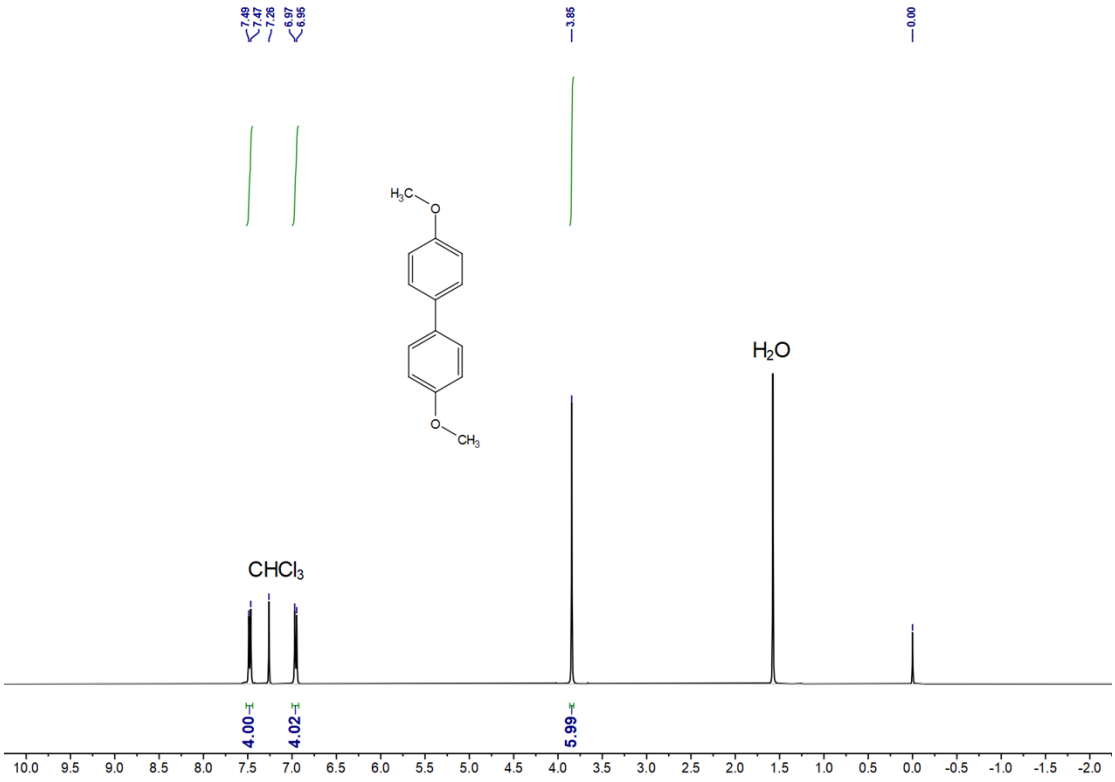

Fig. S1. ^{1}H NMR spectrum (400 MHz, $CDCl_3$, room temperature) of **2**.

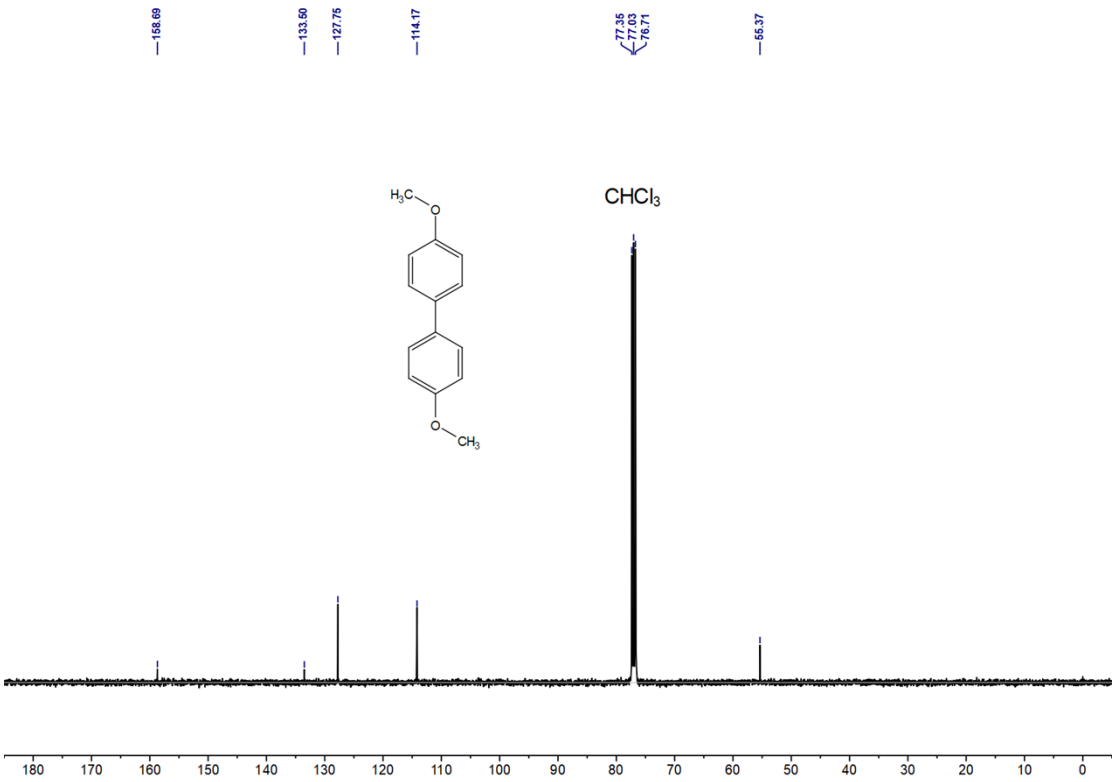

Fig. S2. ^{13}C NMR spectrum (100 MHz, $CDCl_3$, room temperature) of **2**.

*4. Synthesis of **3**[S2]*

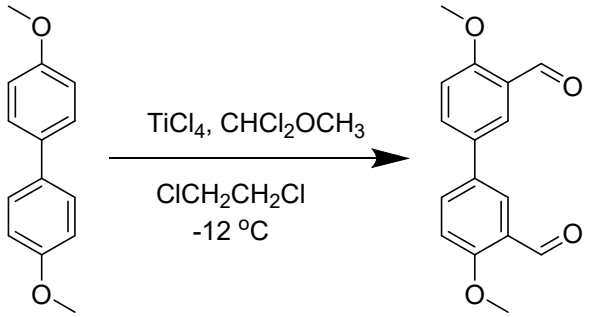

2 **3**

4,4'-Dimethoxybiphenyl **2** (3.00 g, 14 mmol) and DCE (75 ml) were added to a 250 ml round bottom flask, and the solution was cooled to −12 °C with stirring for 15 min. $TiCl_4$ (10.40 ml, 95 mmol) was added carefully, and after stirring for another 1 h, 1,1-dichlorodimethyl ether (8.50 ml, 95 mmol) was introduced. The reaction mixture was stirred for 30 min at −12 °C, and then slowly warmed to room temperature and stirred overnight before turning dark red. The reaction was quenched by adding 10% HCl (50 mL), and the resulting solid was collected by filtration, which was further purified by recrystallization with dichloromethane and petroleum ether to give **3** as a pale yellow

solid (3.60 g, 95%), M.p. 223.9–226.5 °C.^{1}H NMR (400 MHz, $CDCl_3$, room temperature) δ(ppm): 10.51 (s, 2H), 8.04 (d, J = 2.5 Hz, 2H), 7.80 (dd, J = 8.7, 2.5 Hz, 2H), 7.08 (d, J = 8.7 Hz, 2H), 3.98 (s, 6H). ^{13}C NMR (100 MHz, $CDCl_3$, room temperature) δ(ppm):189.73, 161.26, 133.97, 132.16, 126.32, 124.90, 112.30, 77.24, 55.91.

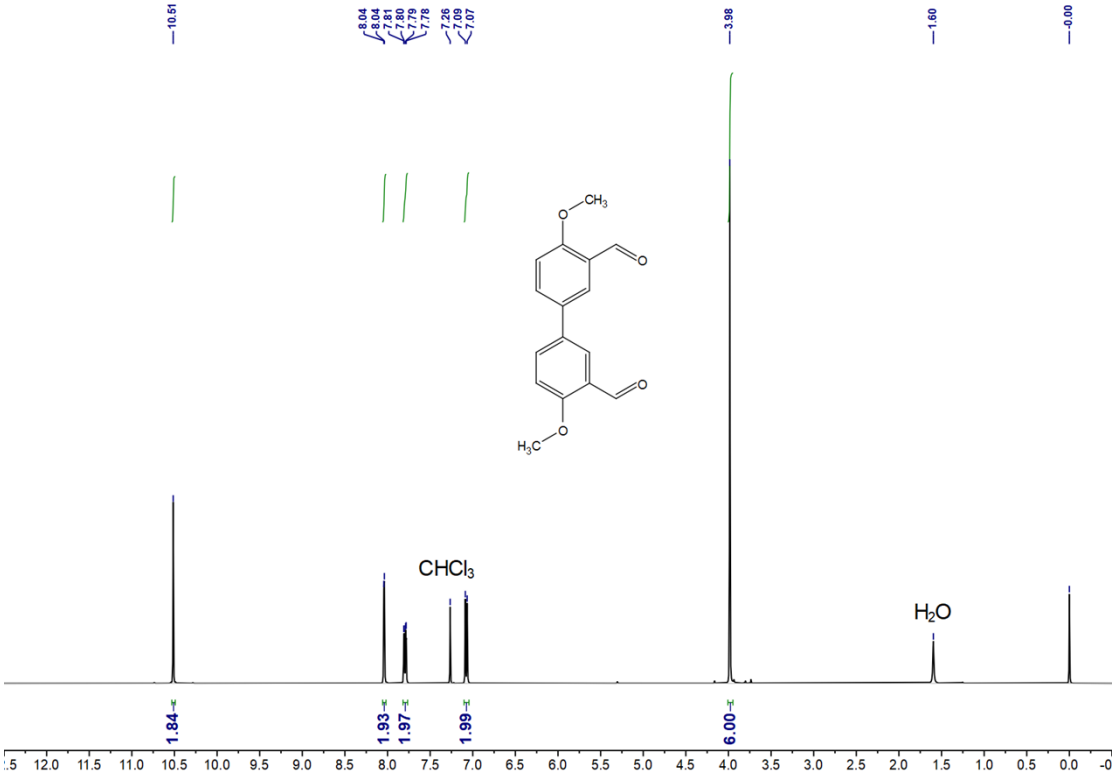

Fig. S3. ^{1}H NMR spectrum (400 MHz, $CDCl_3$, room temperature) of **3**.

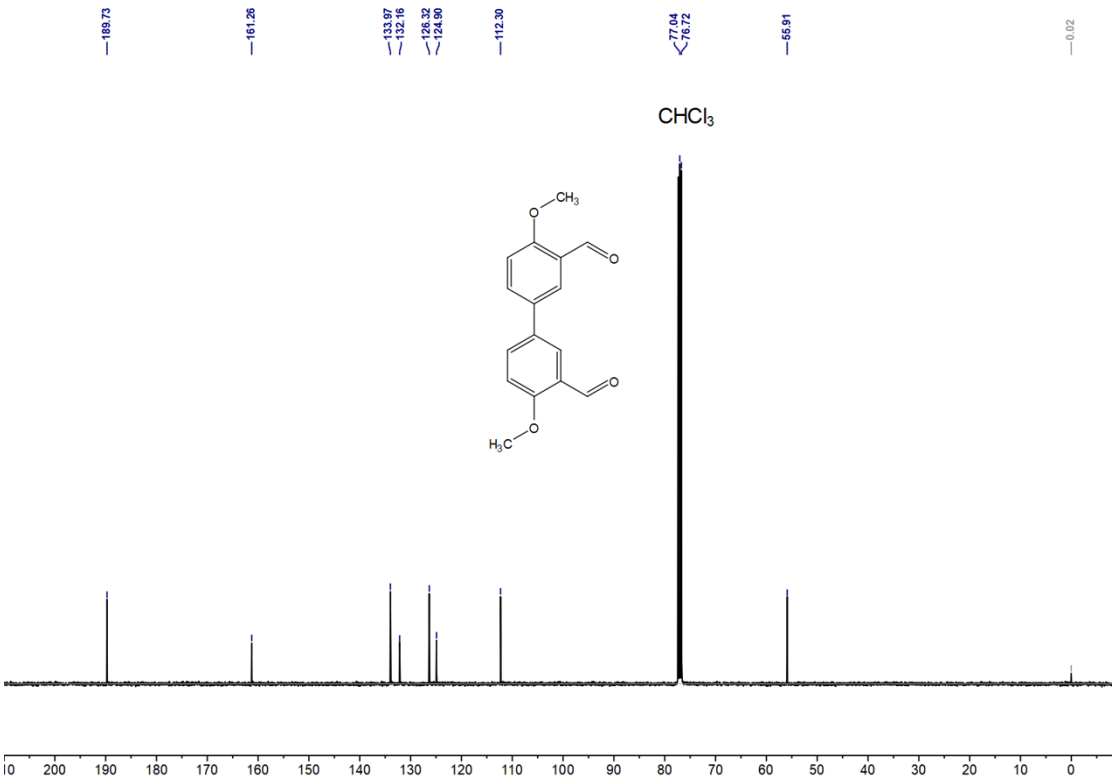

Fig. S4. ^{13}C NMR spectrum (100 MHz, $CDCl_3$, room temperature) of **3**.

*5. Synthesis of **4**[S3]*

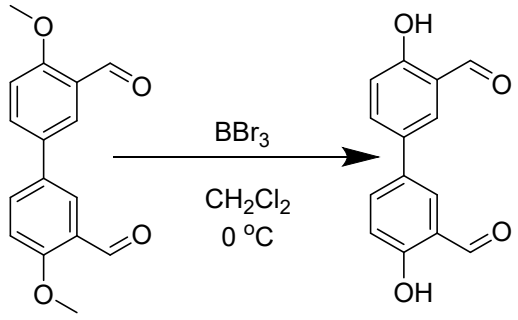

3 **4**

To a 250 ml round-bottomed flask were added 4,4′-dimethoxy[1,1′-biphenyl]-3,3′-dicarboxaldehyde **3** (0.83 g, 3.07 mmol) and DCM (50 ml). After the solution was cooled to 0 °C, BBr_3 (0.71 ml, 7.39 mmol) was added. Continue stirring for 6 h; it was quenched with H_2O, and a yellow solid was precipitated after stirring for 30 min. The solid was collected by filtration and washed with acetone to give **4** as a yellow solid (0.69 g, 93%), M.p. 237.1–242.6 °C.^{1}H NMR (400 MHz, $CDCl_3$, room temperature) δ (ppm): 11.01 (s, 2H), 9.99 (s, J = 6.7 Hz 2H), 7.73 (d, 4H), 7.10 (d, J = 9.3 Hz, 2H).

^{13}C NMR (100 MHz, $CDCl_3$, room temperature) δ (ppm): 196.49, 161.04, 135.22, 131.58, 131.35, 120.78, 118.49.

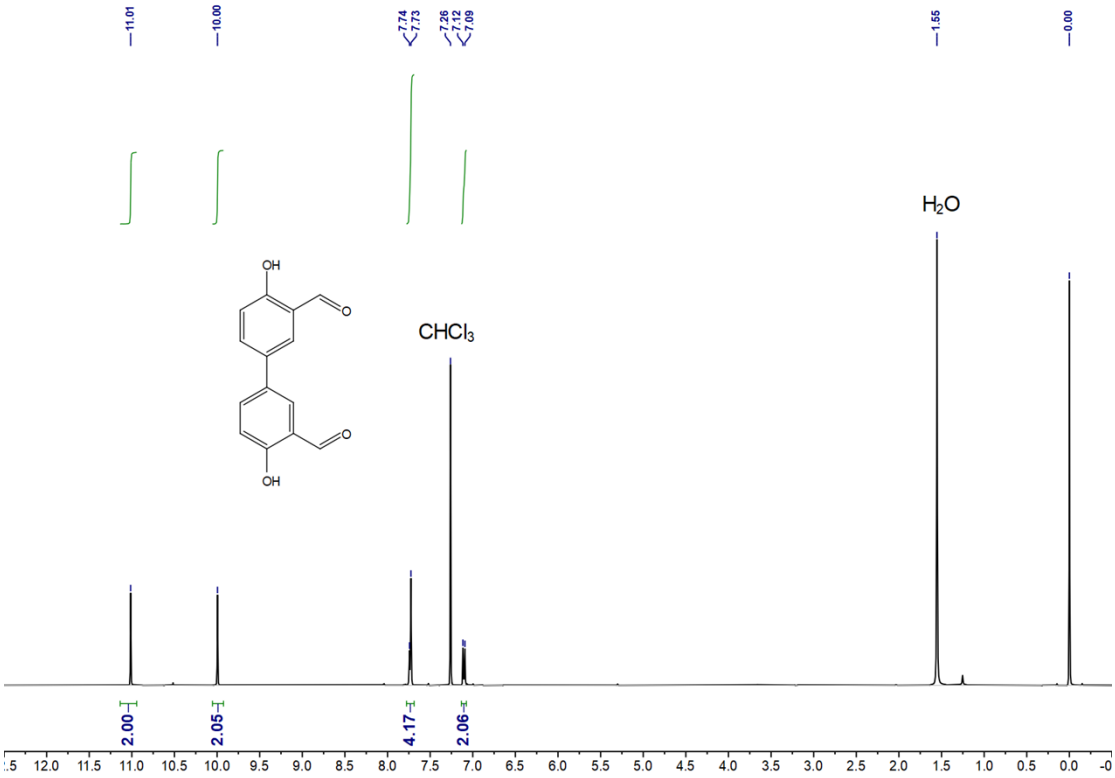

Fig. S5. ^{1}H NMR spectrum (400 MHz, $CDCl_3$, room temperature) of **4**.

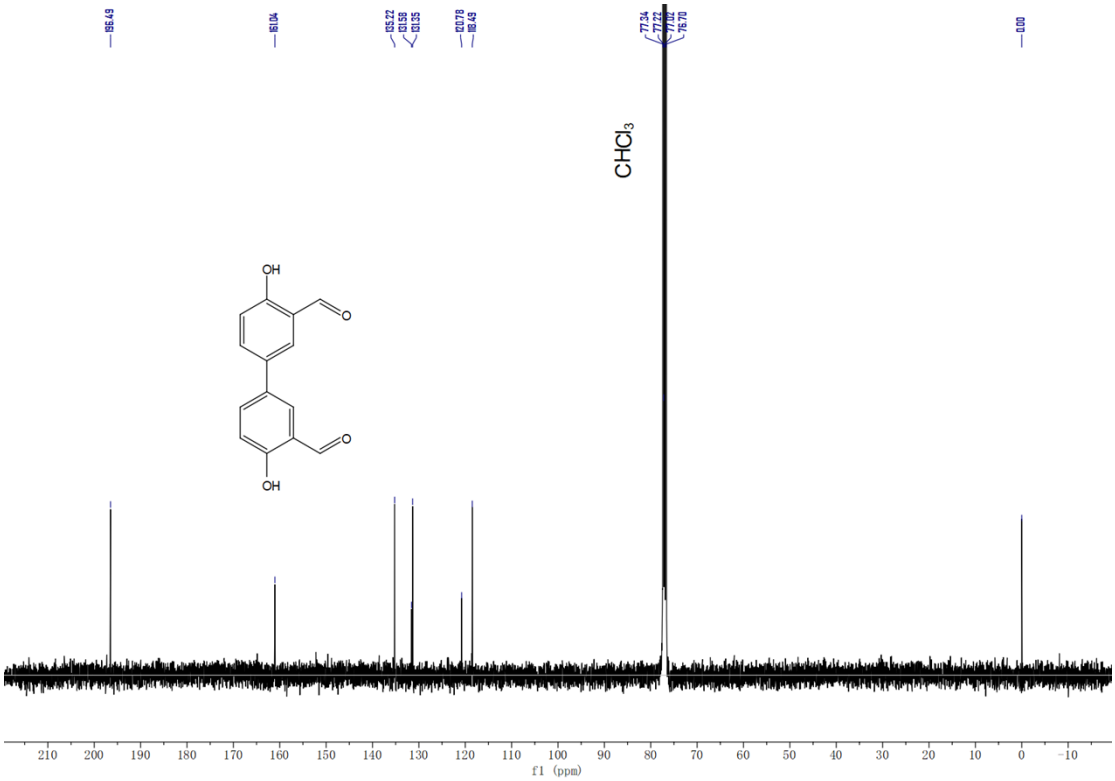

Fig. S6. ^{13}C NMR spectrum (100 MHz, $CDCl_3$, room temperature) of **4**.

6. Synthesis of ***6***[S4, 5]

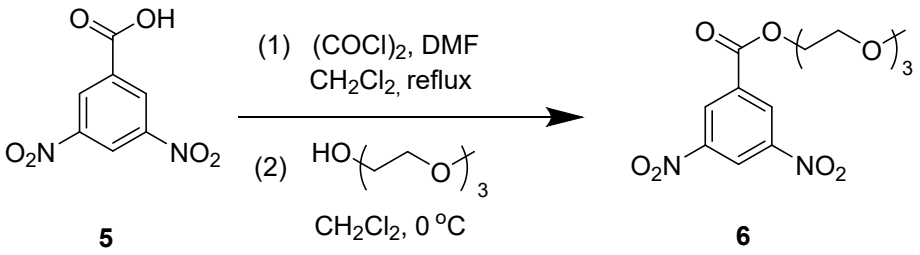

A 250 ml three-necked flask was charged with 3,5- dinitrobenzoic acid **5** (4.24 g, 20 mmol), oxalyl chloride (3.40 ml, 40 mmol), and DCM (100 ml). Then, two drops of DMF were added to the stirring solution, and the mixture was refluxed for 4 h. The solvent was removed in vacuo and dried in a vacuum drying oven to give 3,5-dinitrobenzoyl chloride (4.26 g, 93%) which was used directly in the next step.

In a 250 ml round bottom flask, 3,5-dinitro benzoyl chloride (4.26 g, 18.48 mmol) was dissolved in DCM (100 ml) at 0 °C, triethylene glycol monomethyl ether (2.67 ml, 16.63 mmol) and triethylamine (10.3 ml, 74 mmol) were added. The mixture was slowly warmed to room temperature and stirred for two days. After that, the solution was poured into the water with stirring and washed with water three times. The residue was partitioned between DCM and saturated $NaHCO_3$ three times. The organic layer was collected, dried (Na_2SO_4), and concentrated to give **6** as a brownish-black oil (4.00 g, 91%). ^{1}H NMR (400 MHz, $CDCl_3$, room temperature) δ (ppm): 9.24 (t, J = 2.2 Hz, 1H), 9.19 (d, J = 2.1 Hz, 2H), 4.61 (t, J = 4.7 Hz, 2H), 3.89 (t, J = 4.7 Hz, 2H), 3.76 – 3.63 (m, 6H), 3.54 (dd, J = 5.3, 4.2 Hz, 2H), 3.36 (s, 3H). ^{13}C NMR (100 MHz, $CDCl_3$, room temperature) δ (ppm): 162.56, 148.67, 133.86, 129.58, 122.42, 71.93, 70.70, 70.67, 70.63, 68.78, 65.81, 59.05.

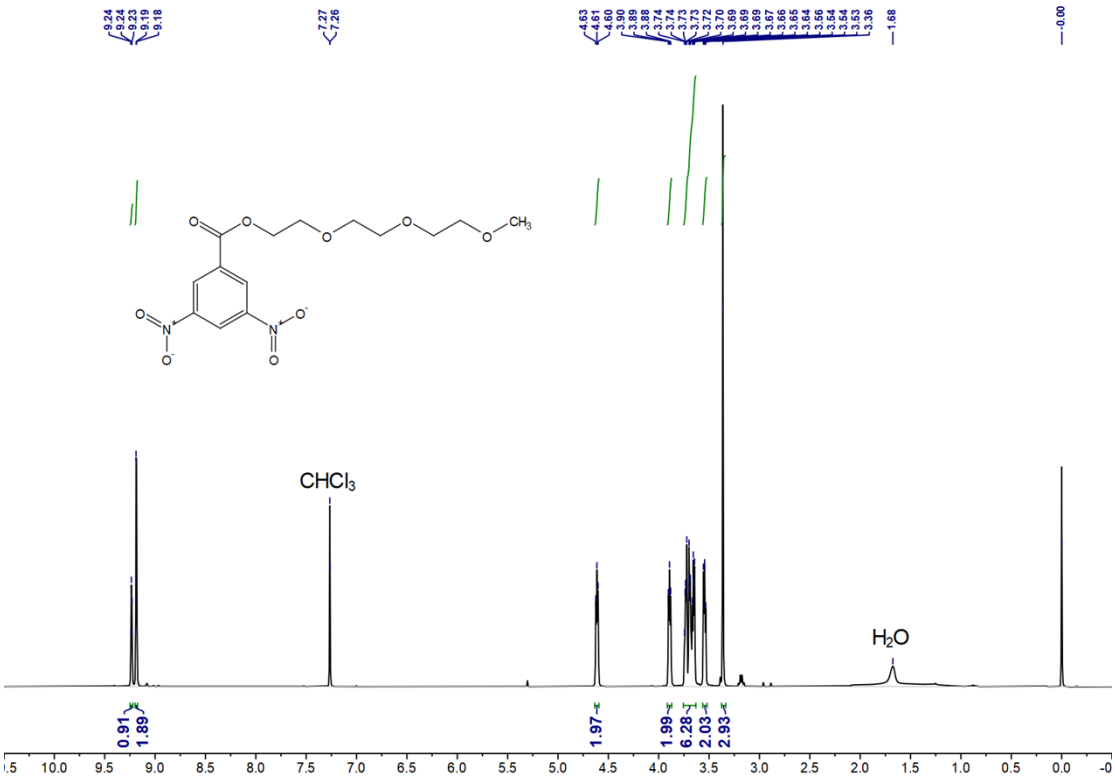

Fig. S7. ^{1}H NMR spectrum (400 MHz, $CDCl_3$, room temperature) of **6**.

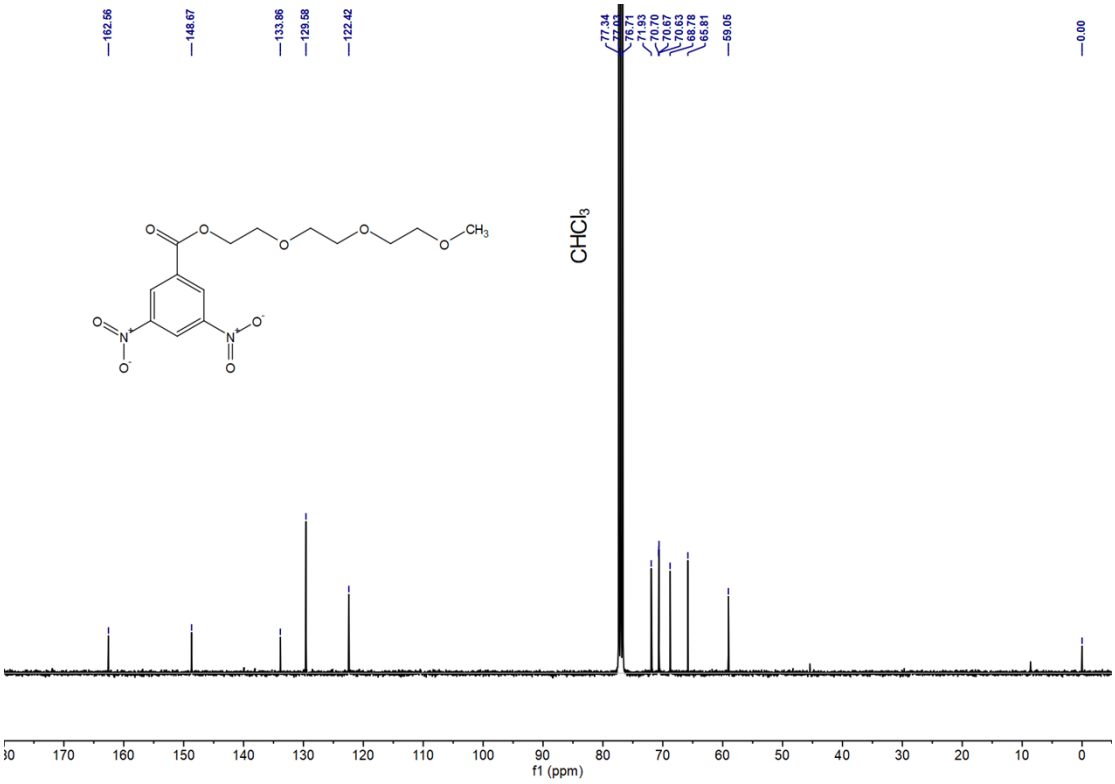

Fig. S8. ^{13}C NMR spectrum (100 MHz, $CDCl_3$, room temperature) of **6**.

7. Synthesis of 7[S6]

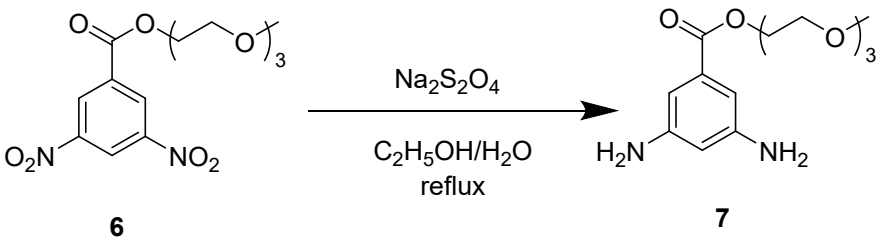

6 **7**

In a 250 ml three-necked flask, 2-[2-(2-methoxyethoxy)ethoxy]-1-(3,5-dinitrobenzene) **6** (4.07 g, 11.84 mmol) was dissolved in a mixed solution of ethanol (120 ml) and H_2O (60 ml). The mixture was added sodium dithionite (10.30 g, 59.2 mmol) in two portions within 2 hours and refluxed for 7 hours. Then, the ethanol was removed in a vacuum before DCM (30 ml) and saturated $NaHCO_3$ (30 mL) were added. After stirred for 30 min, the organic layer was separated, dried, and concentrated to give **7** as a yellow oil (1.09 g, 31%). ^{1}H NMR (400 MHz, $CDCl_3$, room temperature) δ (ppm): 6.80 (d, J = 2.1 Hz, 2H), 6.19 (t, J = 2.1 Hz, 1H), 4.42 (t, J = 4.8 Hz, 2H), 3.81 (t, J = 4.8 Hz, 2H), 3.70–3.64 (m, 6H), 3.56–3.53 (m, 2H), 3.37 (s, 3H). ^{13}C NMR (100 MHz, $CDCl_3$, room temperature) δ (ppm): 166.82, 147.46, 132.03, 107.07, 105.71, 71.96, 70.74, 70.66, 70.63, 69.27, 63.99, 59.03.

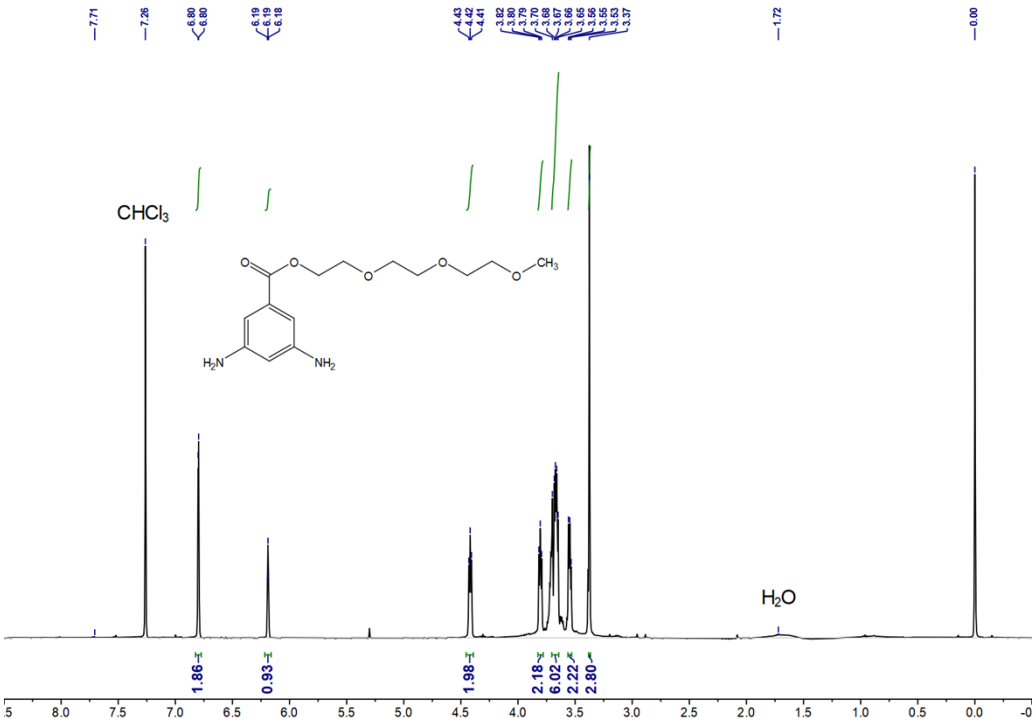

Fig. S9. ^{1}H NMR spectrum (400 MHz, $CDCl_3$, room temperature) of **7.**

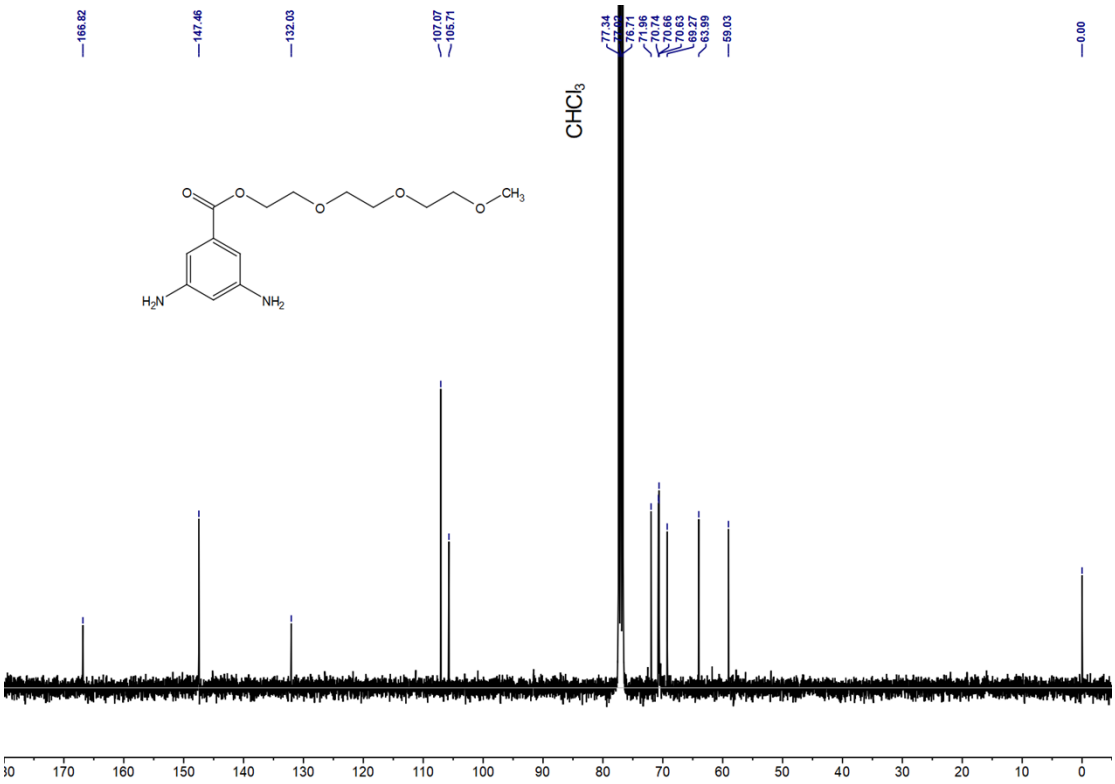

Fig. S10. ^{13}C NMR spectrum (100 MHz, $CDCl_3$, room temperature) of **7**.

*8. Synthesis of **MR**[S7]*

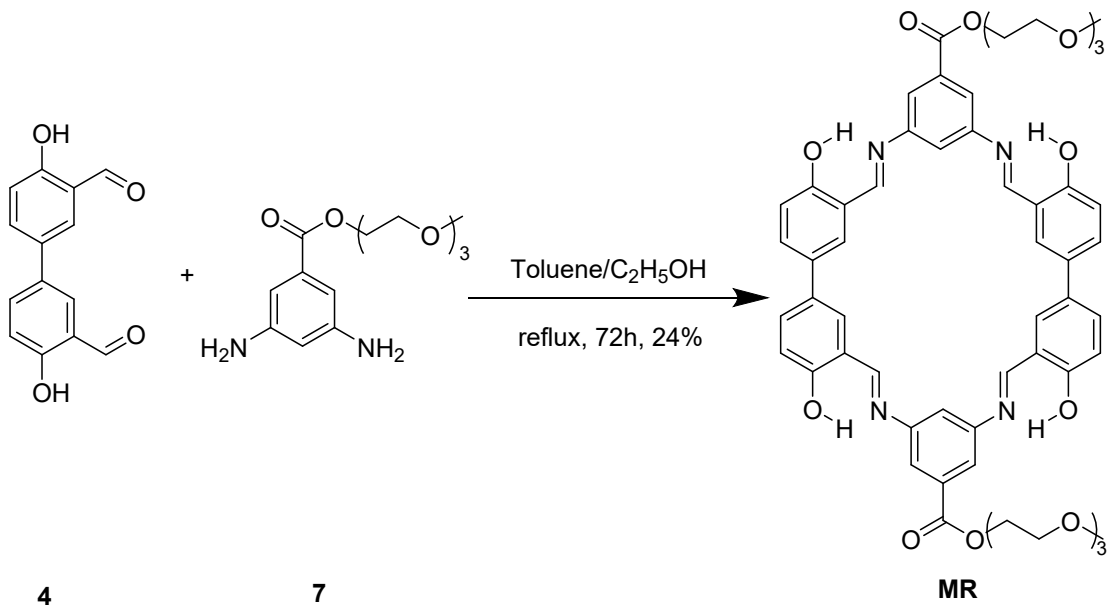

2-(2-(2-Methoxyethoxy)ethoxy)ethyl 3,5-diaminobenzoate **7** (0.92 g, 3.08 mmol) and 4,4′-dihydroxy[1,1′-biphenyl]-3,3′-dicarboxaldehyde **4** (0. 39 g, 1.62 mmol) were heated at reflux in toluene (100 mL) and ethanol (20 mL) under Dean-Stark conditions. After 72 h, the reaction mixture was cooled to room temperature, and the precipitate

was collected by filtration and washed with ethanol to produce an orange-red solid **MR** (0.80 g, 24%). M.p. > 262 °C. ^{1}H NMR (400 MHz, $CDCl_3$, room temperature) δ(ppm): 12.47 (s, 4H), 8.93 (s, 4H), 8.04 (s, 4H), 7.81 (s, 4H), 7.72 (d, J = 8.8 Hz, 4H), 7.45 (s, 2H), 7.17 (d, J = 8.6 Hz, 4H), 4.55 (d, J = 5.1 Hz, 4H), 3.89 (d, J = 5.2 Hz, 4H), 3.76 – 3.66 (m, 12H), 3.56 (t, J = 4.8 Hz, 4H), 3.37 (s, 6H). ^{13}C NMR (100 MHz, $CDCl_3$, room temperature) δ(ppm): 165.47, 163.99, 160.25, 150.15, 131.47, 131.08, 130.65, 125.20, 119.17, 118.09, 109.74, 71.94, 70.72, 70.69, 70.64, 69.16, 64.71, 59.05. HRESIMS: m/z calcd for $[M + Na]^+$ $C_{56}H_{56}N_4NaO_{14}$, 1031.3685, found 1031.3691, error 0.6 ppm.

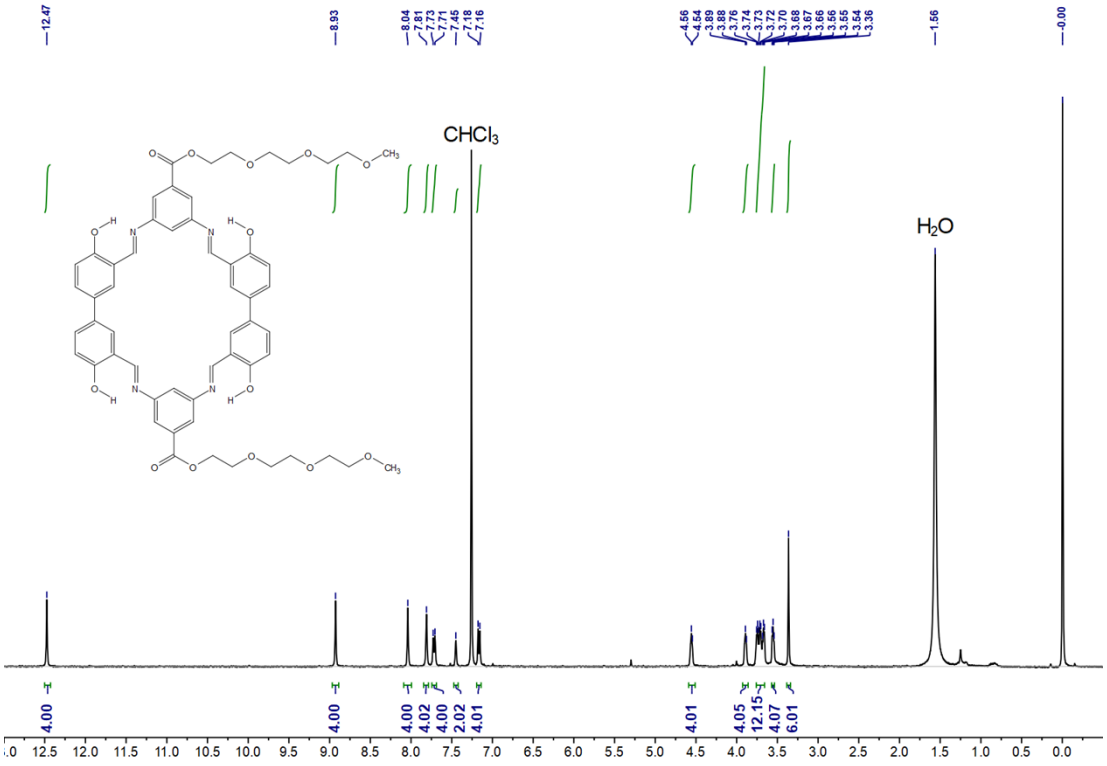

Fig. S11. ^{1}H NMR spectrum (400 MHz, $CDCl_3$, room temperature) of **MR.**

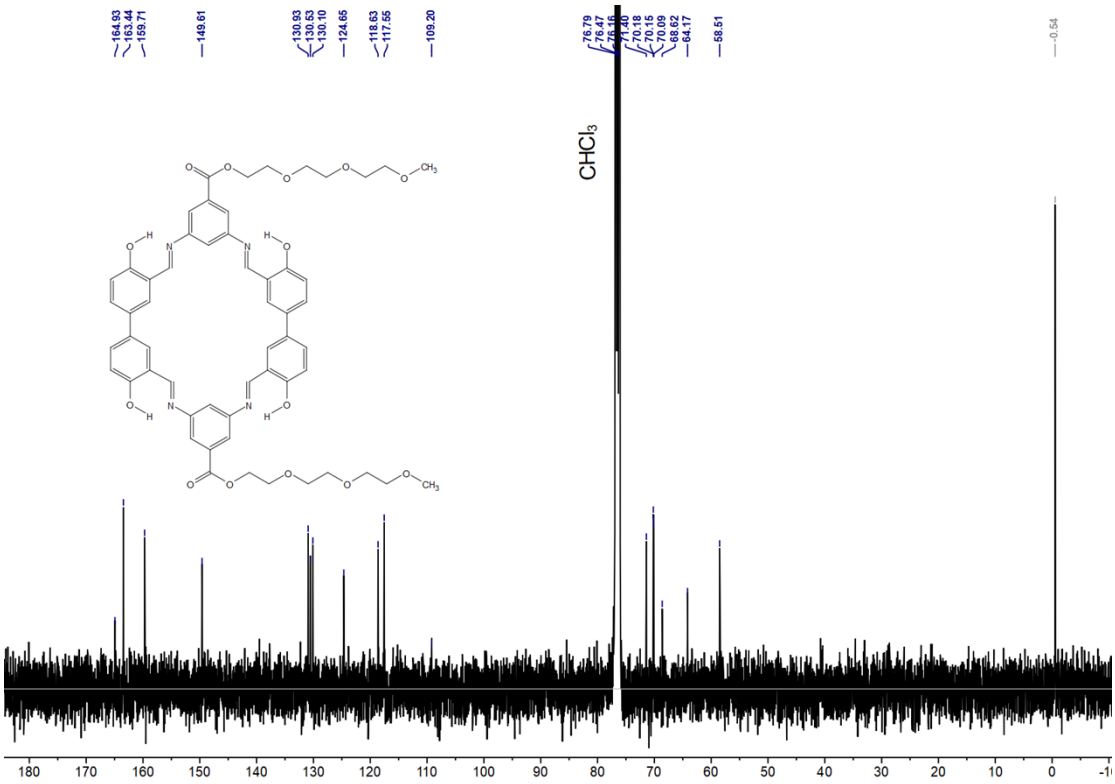

Fig. S12. ^{13}C NMR spectrum (100 MHz, $CDCl_3$, room temperature) of **MR**.

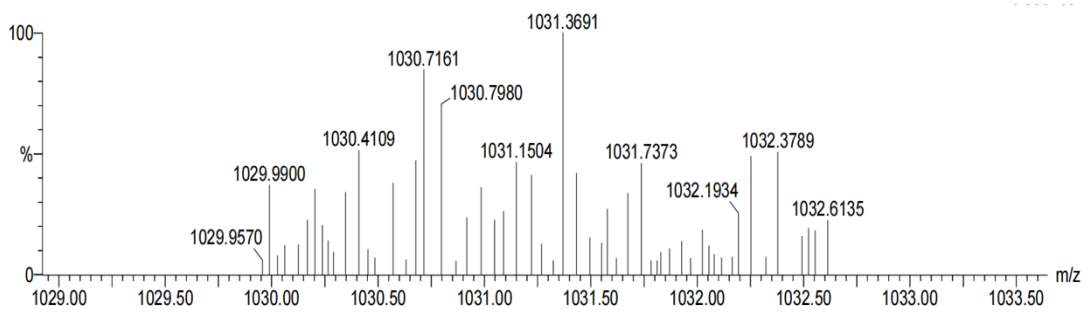

Fig. S13. Electrospray ionization mass spectrum of **MR**. Assignment of the main peak: m/z 1031.3691 $[M + Na]^+$ (100%).

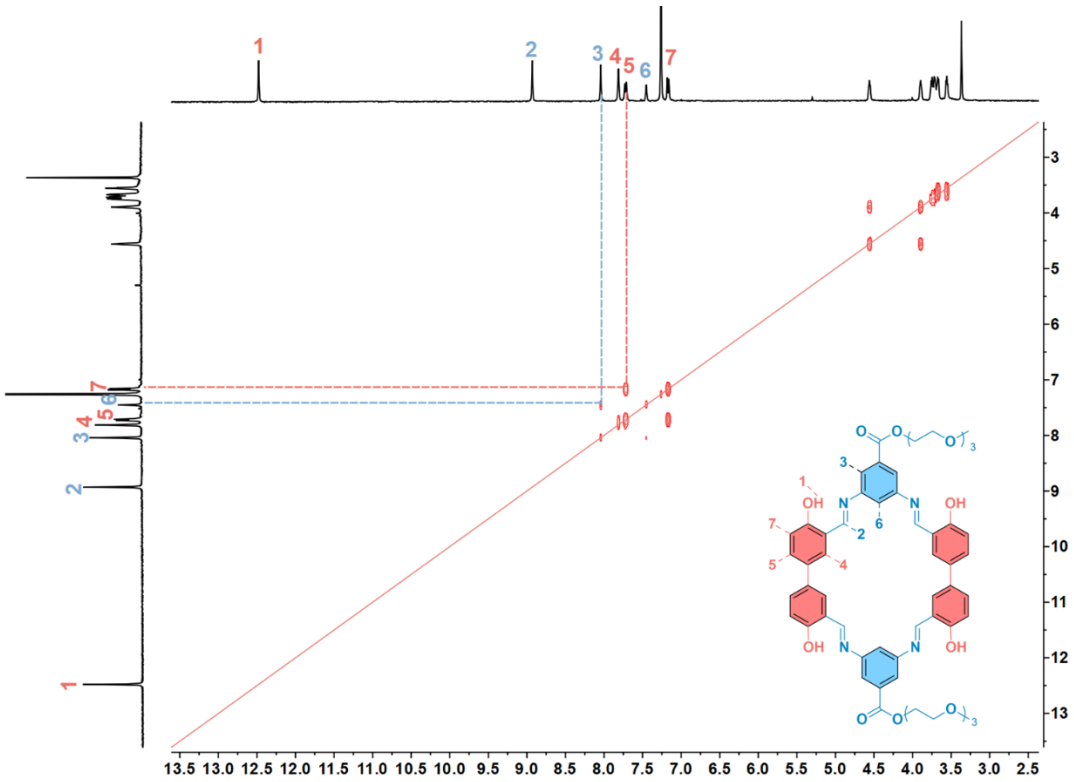

Fig. S14. 2D COSY spectrum of **MR** in $CDCl_3$ at room temperature.

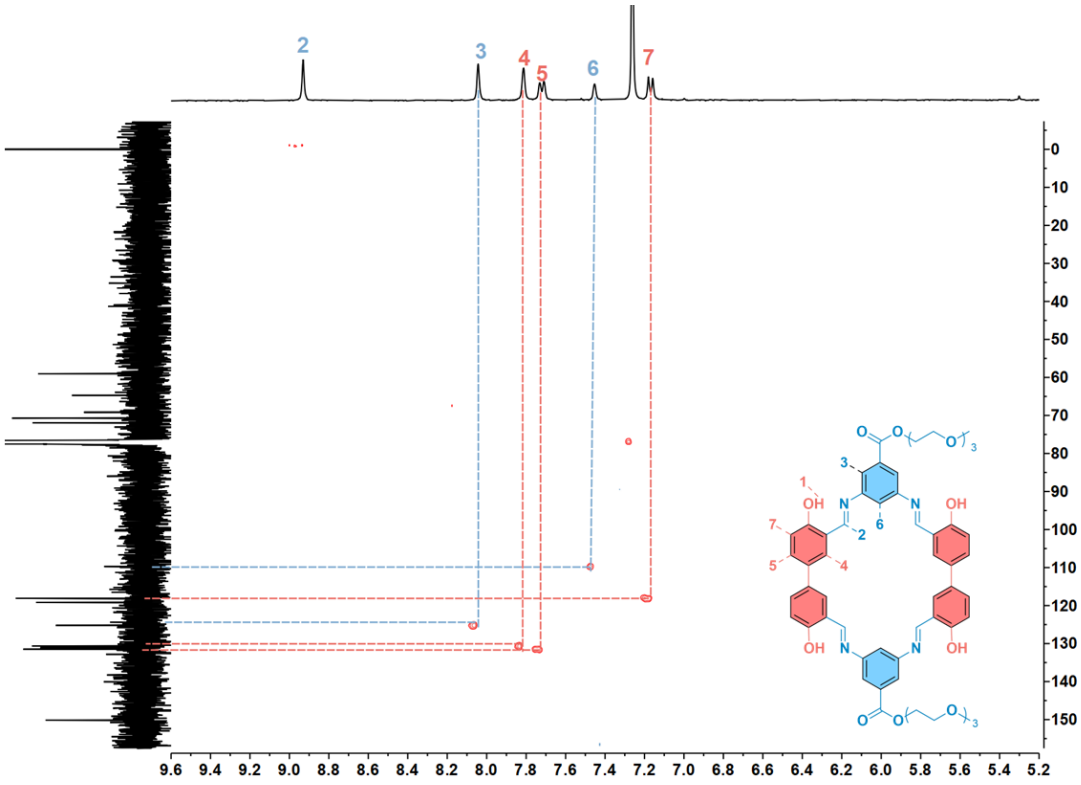

Fig. S15. 2D HSQC partial spectrum of **MR** in $CDCl_3$ at room temperature.

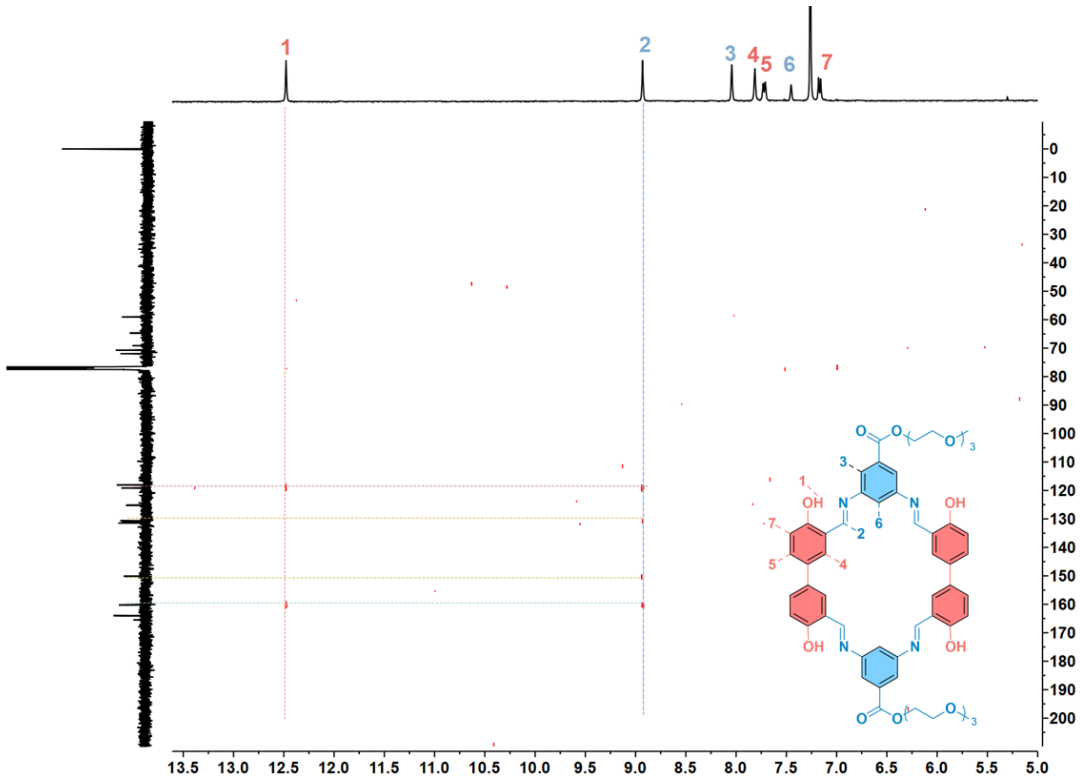

Fig. S16. 2D HMBC partial spectrum of **MR** in $CDCl_3$ at room temperature.

*9. ^1H NMR spectra of **MR** in $CDCl_3$ and DMSO-d_6*

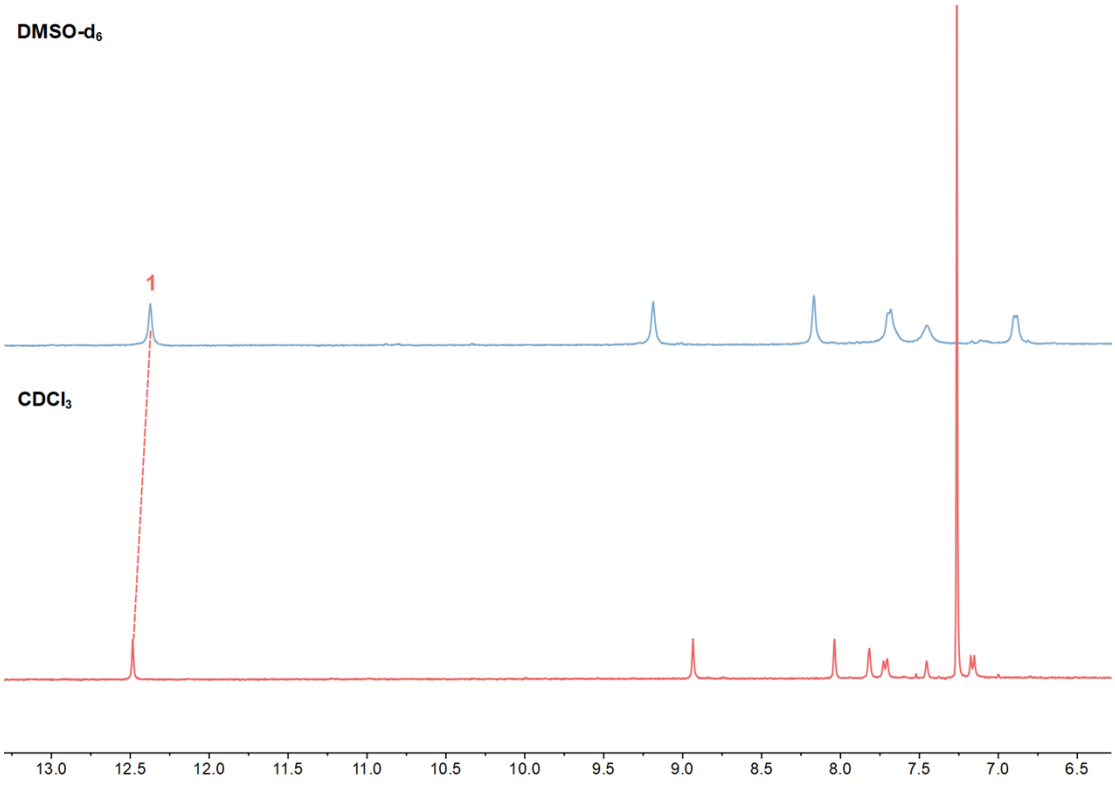

Fig. S17. Partial ^{1}H NMR spectra (400 MHz, room temperature) of **MR** in $CDCl_3$ and DMSO-d_6.

*10. Partial ^{1}H NMR spectra of **MR** with various equivalents of TBAX (X=Cl, Br and I)*

^{1}H NMR titrations were done with a constant concentration of **MR** (2 mM) and varying concentrations of *TBAX*.

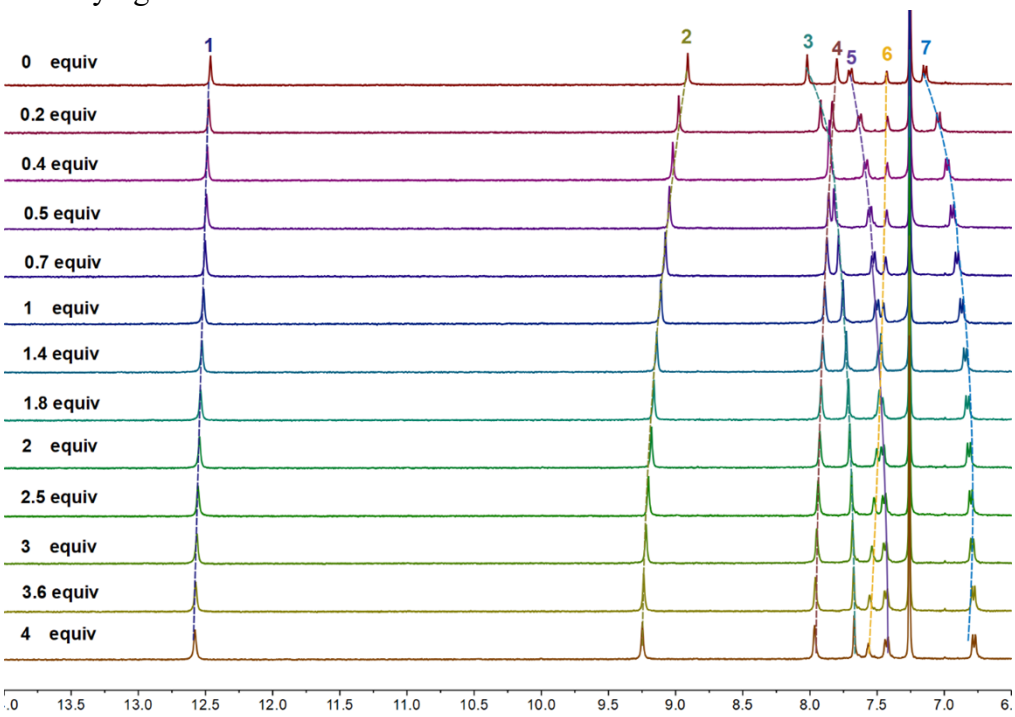

Fig. S18. Partial ^{1}H NMR spectra (400 MHz, $CDCl_3$, room temperature) of **MR** at the concentration of 2.00 mM upon addition of various equivalents of TBACl (G1).

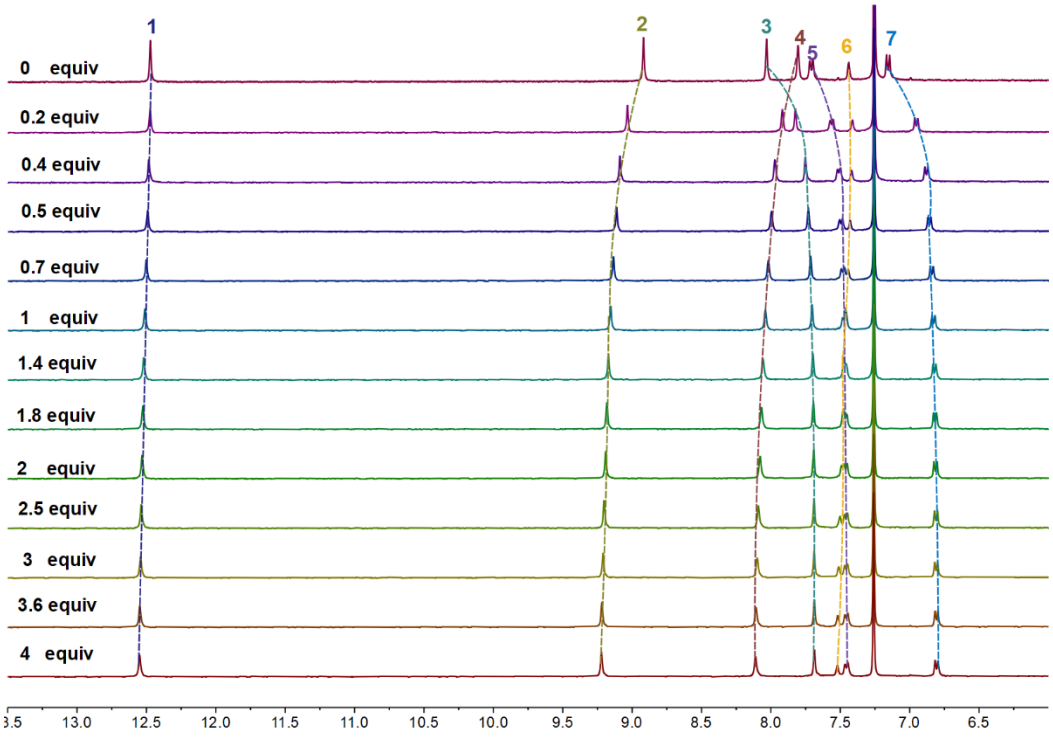

Fig. S19. Partial ^{1}H NMR spectra (400 MHz, $CDCl_3$, room temperature) of **MR** at a the concentration of 2.00 mM upon the addition of various equivalents of TBABr (G2).

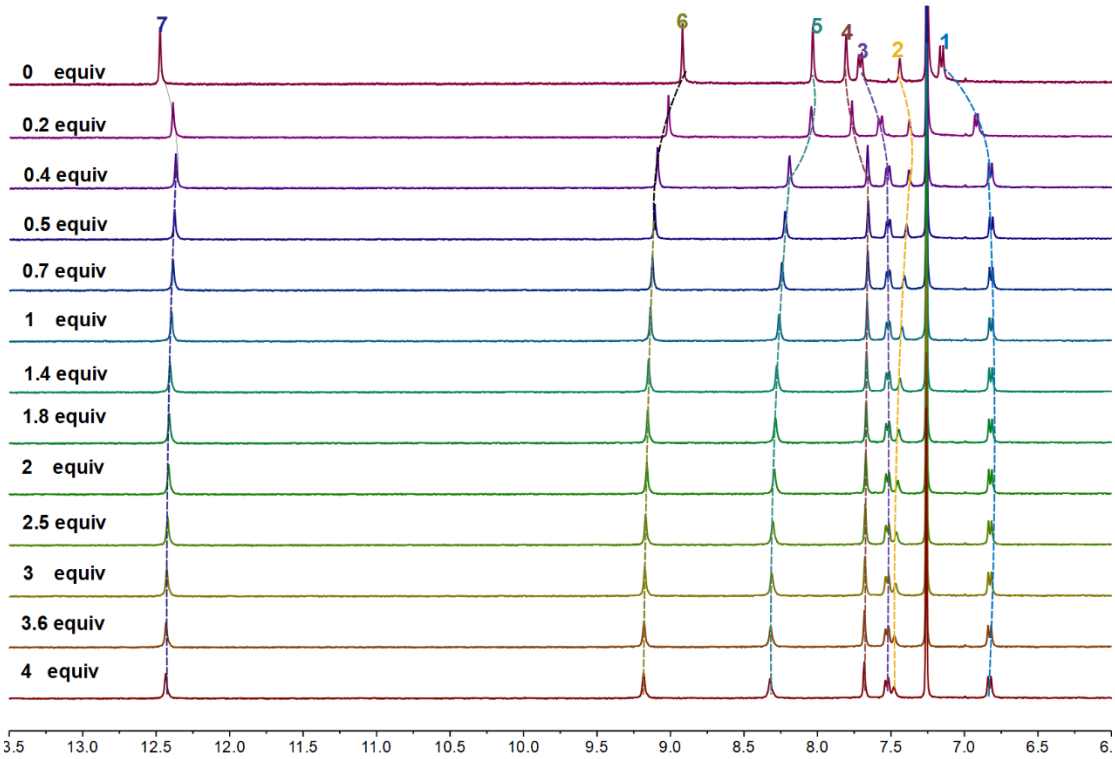

Fig. S20. Partial ^{1}H NMR spectra (400 MHz, $CDCl_3$, room temperature) of **MR** at the concentration of 2.00 mM upon addition of various equivalents of TBAI (G3).

*11. Stoichiometry and association constant determination for the complexations between **MR** and TBAX (X = Cl, Br, and I).*

^{1}H NMR titration experiments determined the stoichiometric and association constants (K_a) between **MR** and TBAX. The association constants (K_a) were estimated to be about 4.82 ± (0.21) × 10^2 M^{-1} for **MR**⊃G1, 1.58± (0.07) × 10^3 M^{-1} for **MR**⊃G2, and 1.95 ± (0.15) × 10^3 M^{-1} for **MR**⊃G3 by the nonlinear curve fitting method. By mole ratio plots, 1:1 stoichiometries were obtained for **MR**⊃G1, **MR**⊃G2 and **MR**⊃G3.

The non-linear curve-fitting was based on the equation:

$$\Delta\delta = (\Delta\delta_\infty/[H]_0)\ (0.5[G]_0 + 0.5([H]_0+1/K_a)–(0.5\ ([G]_0^2+(2[G]_0(1/K_a – [H]_0)) + (1/K_a + [H]_0)^2)^{0.5})) \quad \text{(Eq. S1.)}^{S8}$$

Where $\Delta\delta$ is the chemical shift change of H_2 on **MR** at $[G]_0$, $\Delta\delta_\infty$ is the chemical shift change of H_2 when the host is completely complexed, $[H]_0$ is the fixed initial concentration of the host, and $[G]_0$ is the initial concentration of **G**.

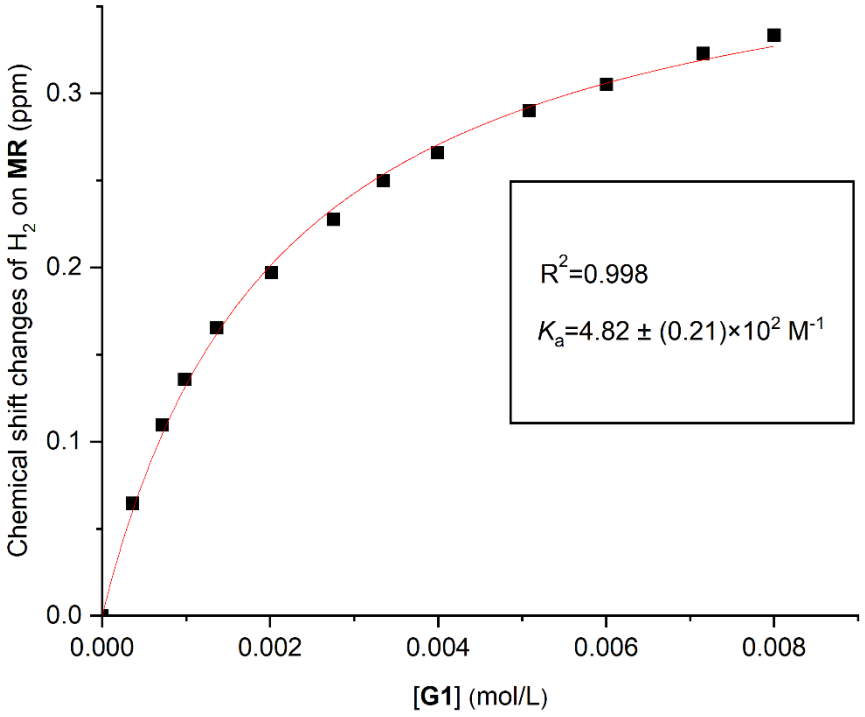

Fig. S21. The chemical shift changes of H_2 on **MR** (2.00 mM) upon the addition of G1 in $CDCl_3$. The red solid line was obtained from the non-linear curve-fitting using Eq. S1.

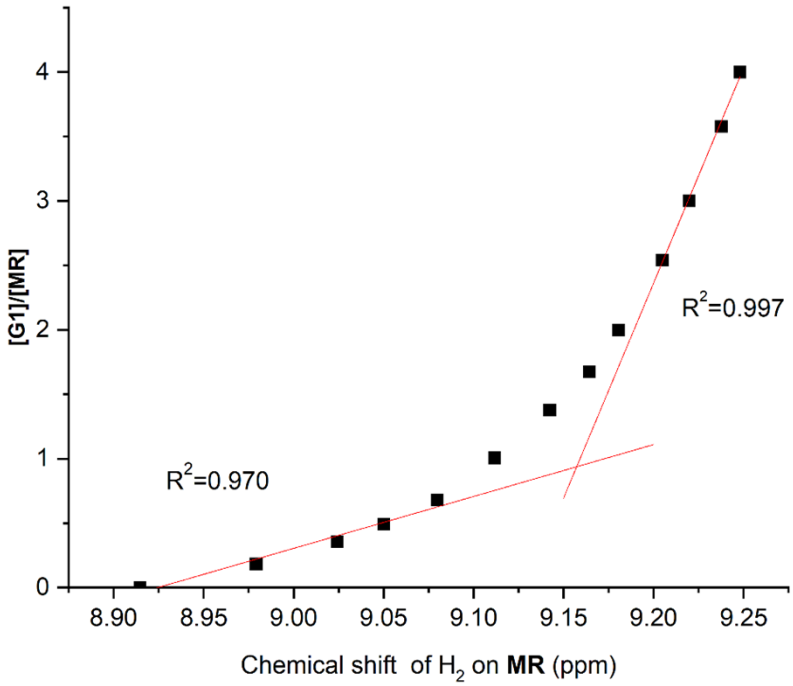

Fig. S22. Mole ratio plot for **MR** and G1, indicating a 1:1 stoichiometry.

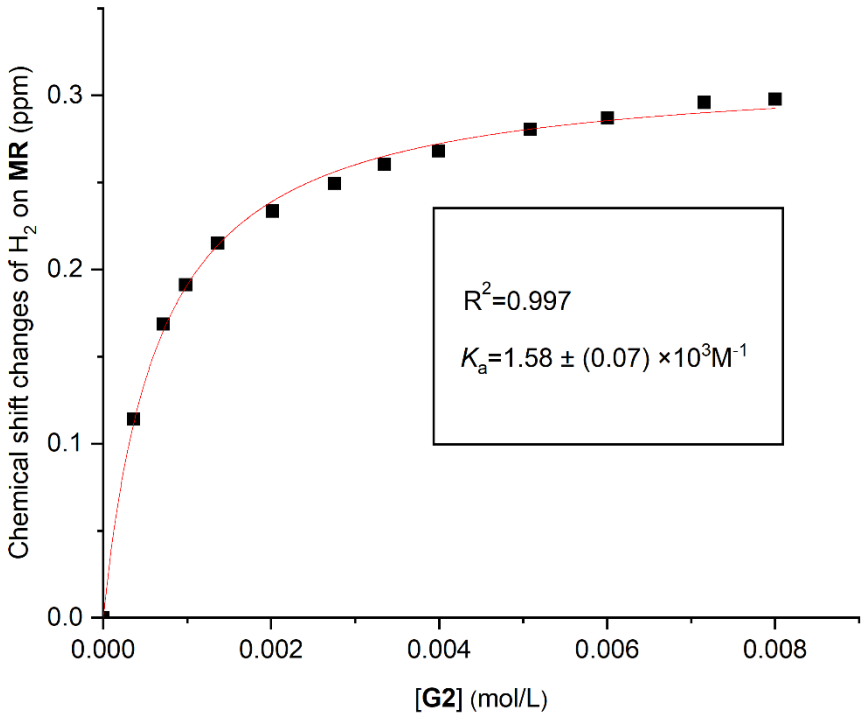

Fig. S23. The chemical shift changes of H_2 on **MR** (2.00 mM) upon the addition of G2 in $CDCl_3$. The red solid line was obtained from the non-linear curve-fitting using Eq. S1.

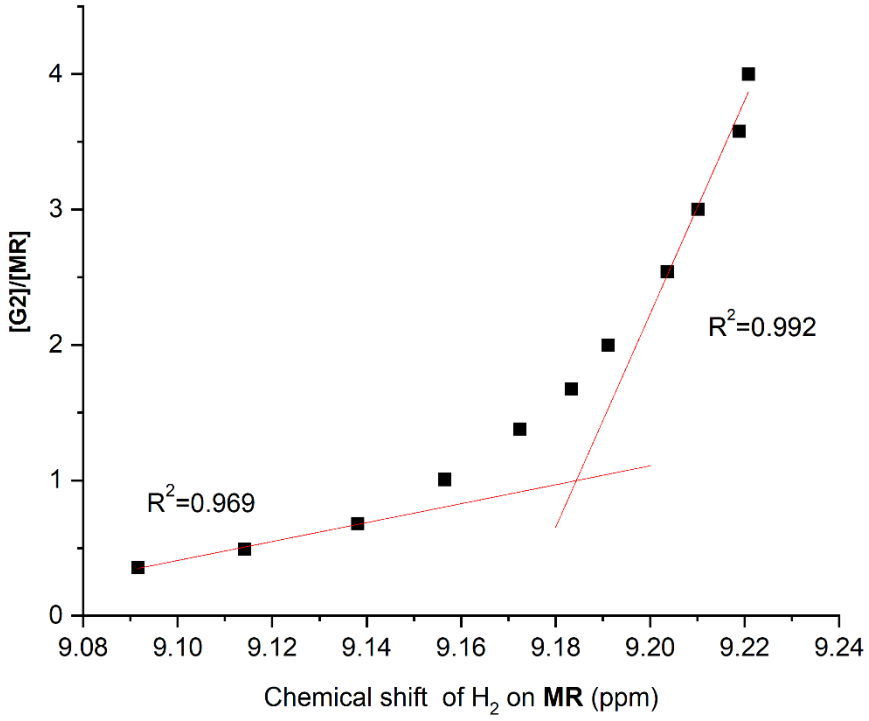

Fig. S24. Mole ratio plot for **MR** and G2, indicating a 1:1 stoichiometry.

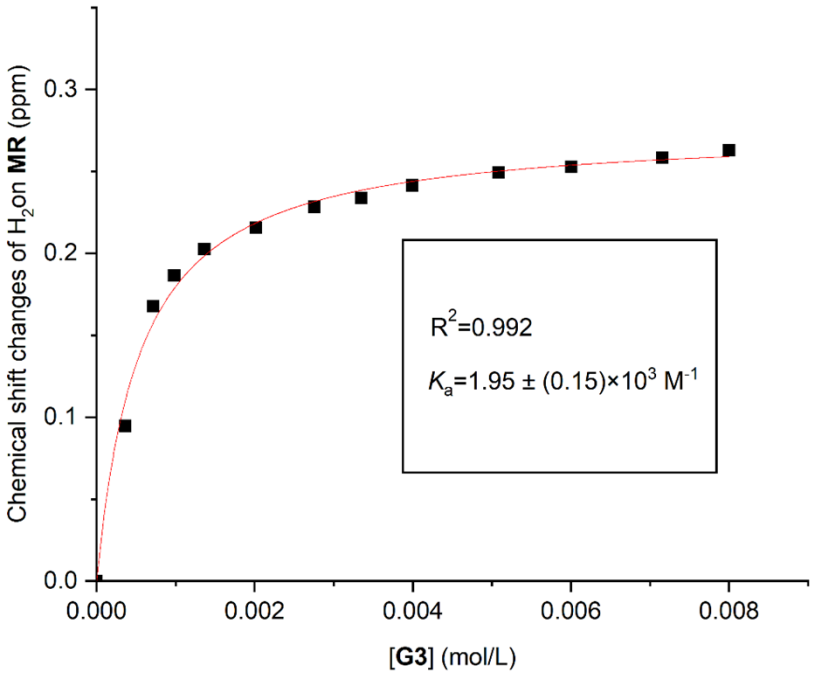

Fig. S25. The chemical shift changes of H_2 on **MR** (2.00 mM) upon the addition of G3 in $CDCl_3$. The red solid line was obtained from the non-linear curve-fitting using Eq. S1.

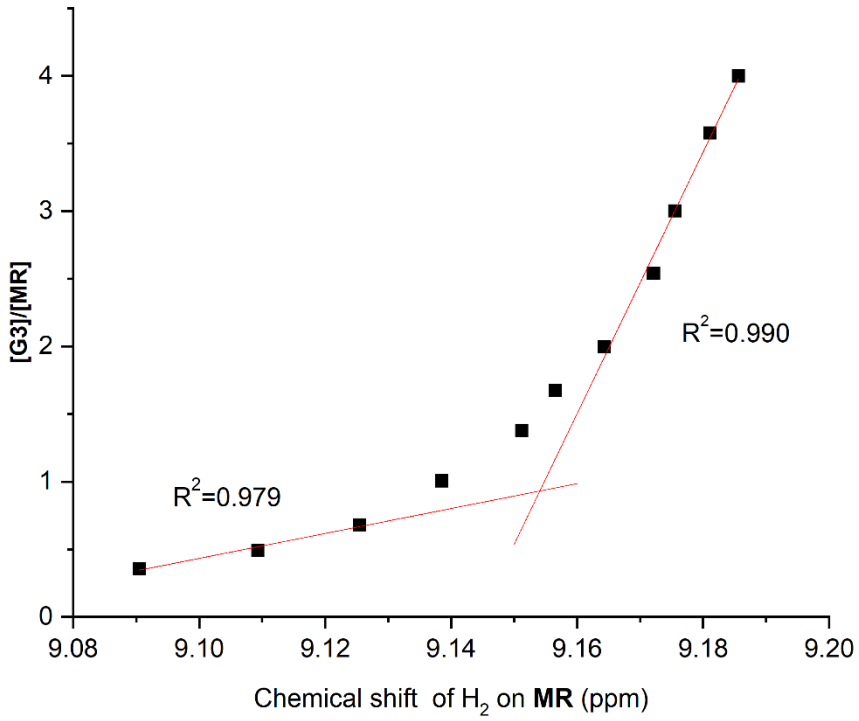

Fig. S26. Mole ratio plot for **MR** and G3, indicating a 1:1 stoichiometry.

*12. Job plots of **MR**⊃TBAX determined by UV-vis spectra*

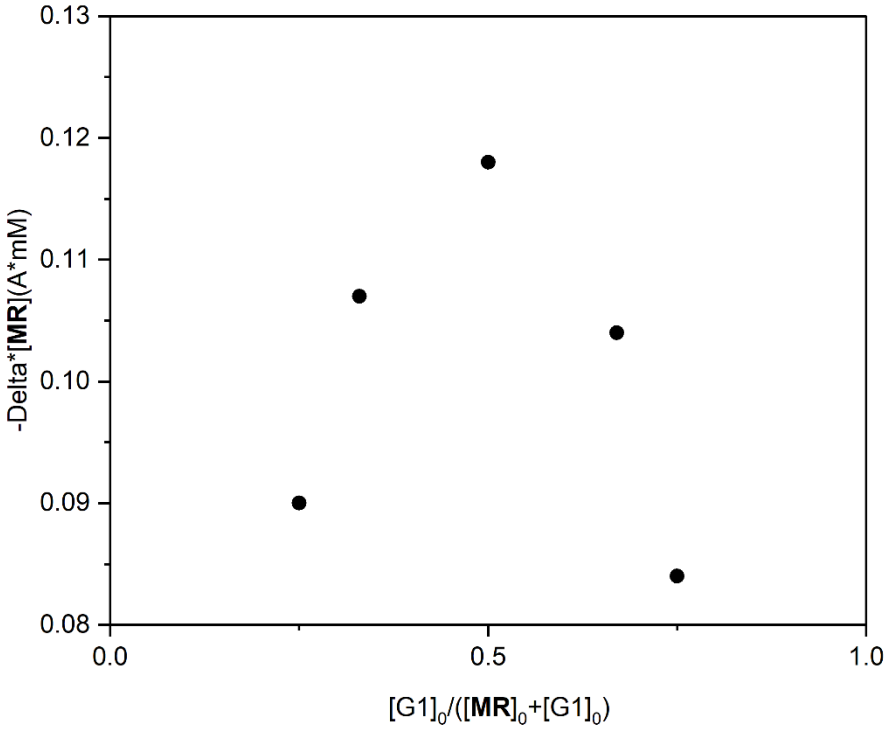

Fig. S27. Job plots of the complex between G1 (TBACl) and **MR** ([host] + [guest] = 0.02 mM) determined by UV-vis spectra. The maximum value was at 0.5, consistent with an 1:1 (host: guest) binding stoichiometry.[S9]

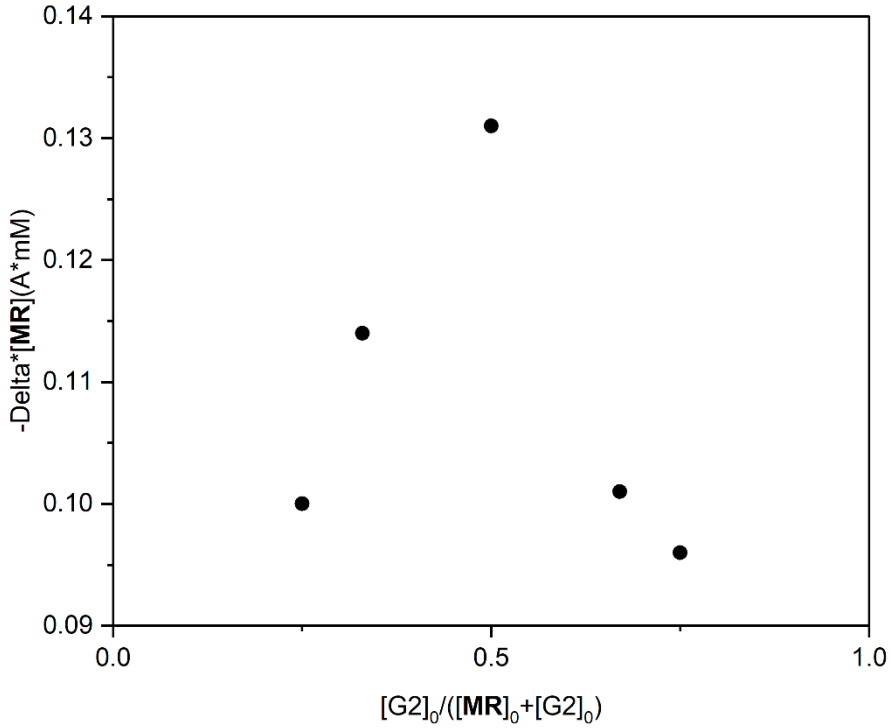

Fig. S28. Job plots of the complex between G2 (TBABr) and **MR** ([host] + [guest] = 0.02 mM) determined by UV-vis spectra. The maximum value was at 0.5, consistent with an 1:1 (host: guest) binding stoichiometry. [S9]

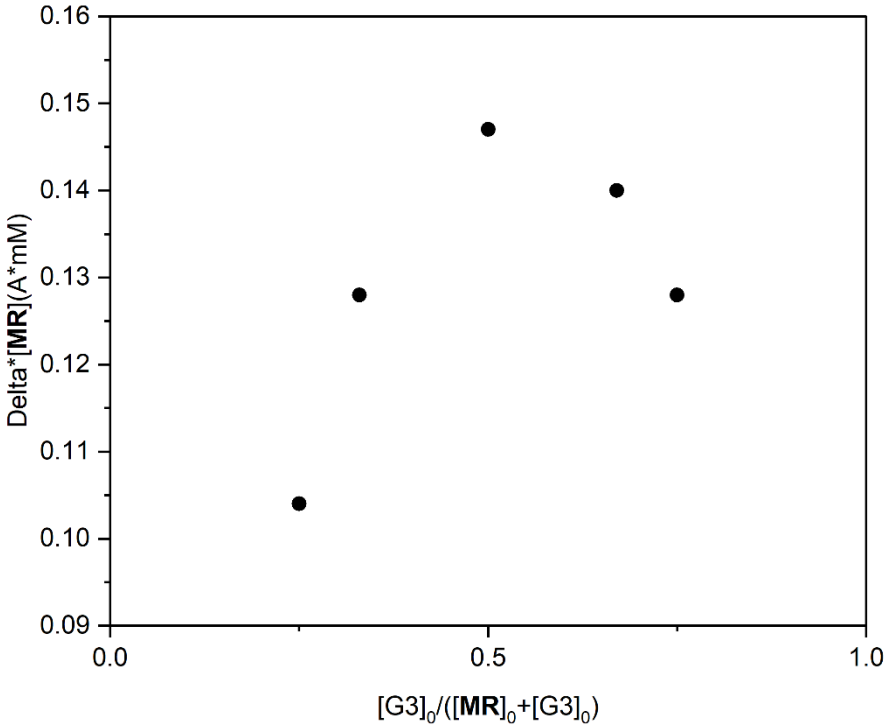

Fig. S29. Job plots of the complex between G3 (TBAI) and **MR** ([host] + [guest] = 0.02 mM) determined by UV-vis spectra. The maximum value was at 0.5, consistent with an 1:1 (host: guest) binding stoichiometry. [S9]

13. *UV-vis spectra of **MR** upon addition of various equivalents of TBABr.*

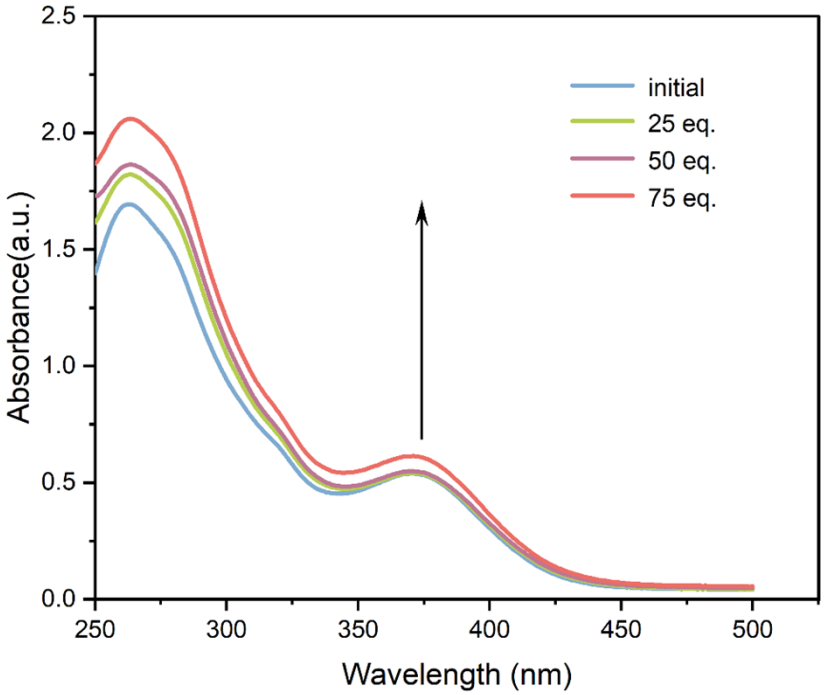

Fig. S30. The UV-vis absorption intensity of **MR** (0.02 mM in $CHCl_3$) varied upon addition of various equivalents of TBABr. The absorption intensity increases with increasing concentration of TBABr.

14. *Fluorescence spectrum of **MR** upon addition of various equivalents of TBABr*

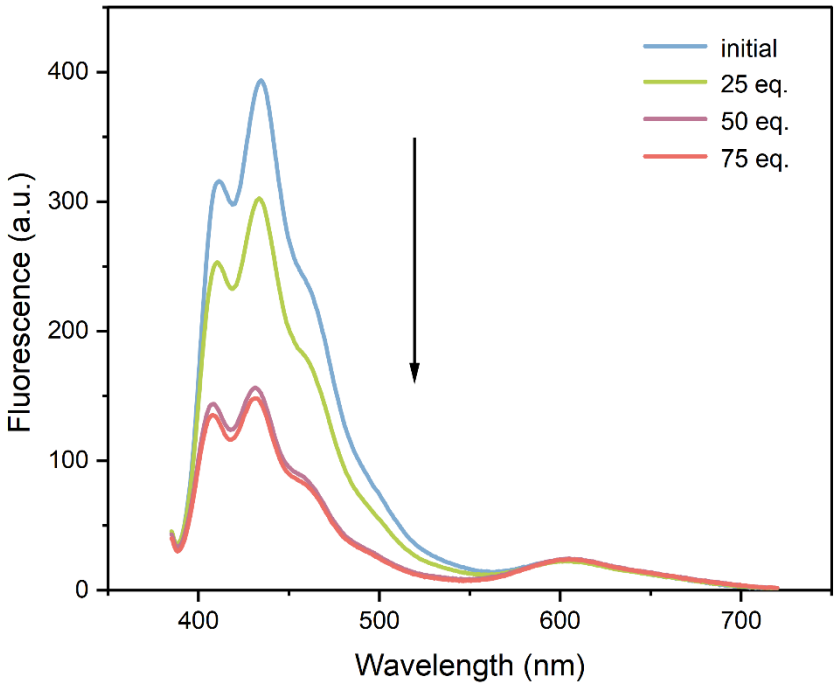

Fig. S31. The fluorescence intensity of **MR** (0.01 mM in $CHCl_3$) changed after addition of different equivalents of TBABr. The fluorescence intensity decreased with increasing TBABr concentration.

*15. Lifetime decay curves and average fluorescence lifetimes of **MR** in $CHCl_3$ and DMSO*

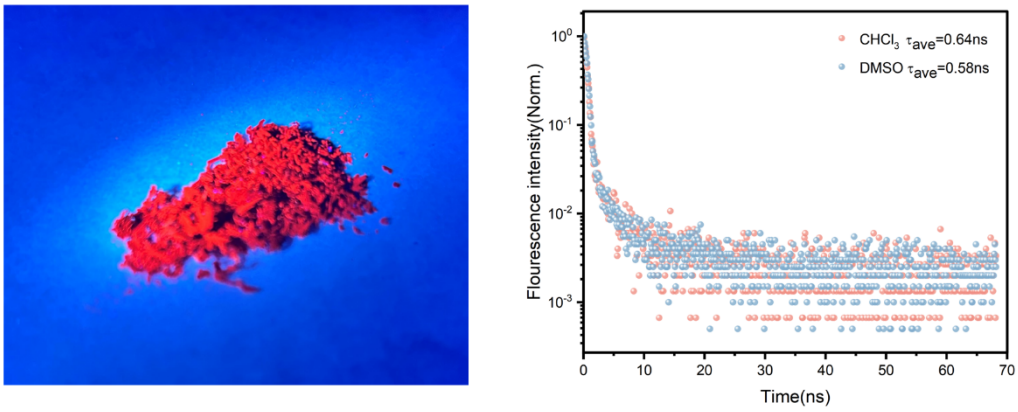

Fig. S32. (a) **MR** fluoresces under a UV laser. (b) Fluorescence lifetime decay curve of **MR** (0.04 mM) in $CHCl_3$ and DMSO.

The average fluorescence lifetimes were based on the equation:

$$\tau = \frac{B_1\tau_1^2 + B_2\tau_2^2}{B_1\tau_1 + B_2\tau_2}$$

Where τ_1 、τ_2 、B_1 and B_2 are substituted into the values of Table S1, they are obtained that the average lifetime of **MR** in $CHCl_3$ was 0.64 ns and the average of **MR** in DMSO was 0.58 ns.

Table S1. Lifetimes and corresponding occupancies of **MR** fitted in $CHCl_3$ and DMSO.

	τ_1	τ_2	B_1	B_2
$CHCl_3$[a]	0.2145	4.9191	0.4670	0.0020
DMSO[a]	0.2254	4.5819	0.4600	0.0020

[a]**MR** (0.04 mM) in $CHCl_3$ and DMSO

*16. Energy-minimizing structure of **MR**.*

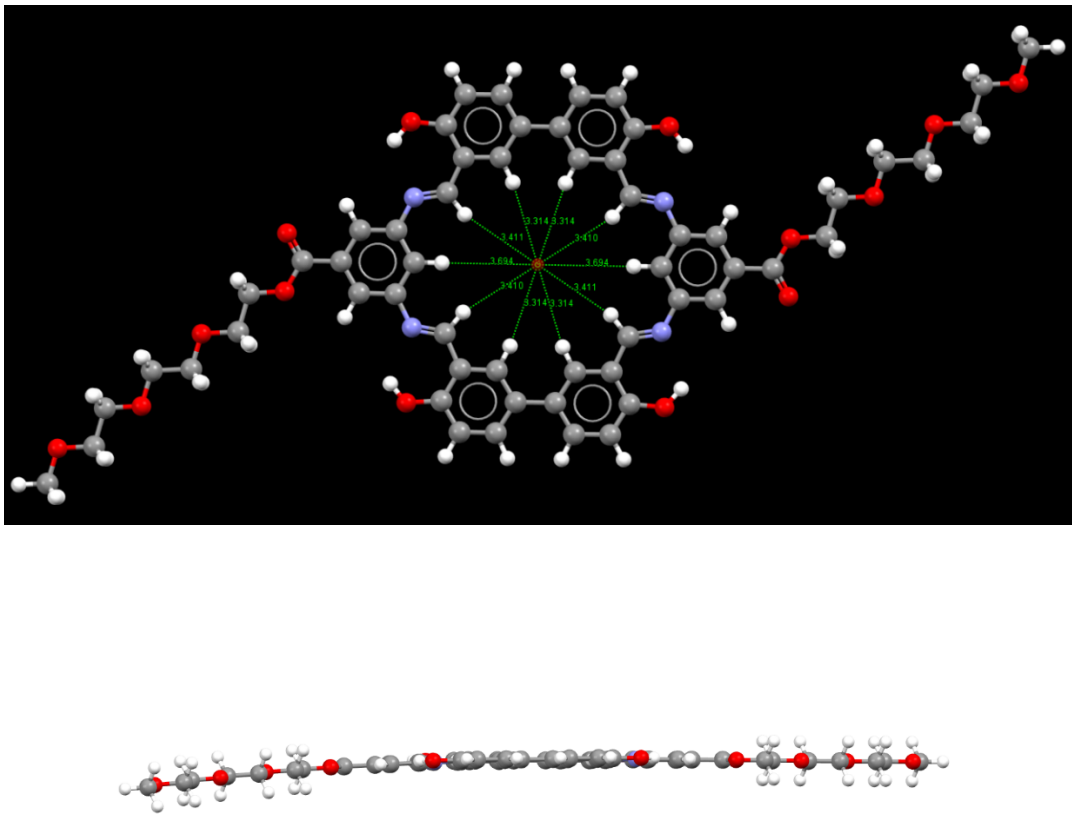

Fig. S33. Energy-minimized structure of MR generated by Avogadro computer program.

The energy-minimized structure of **MR** was calculated (Figure S29), and the minimum distance between the nuclei of the two *para*-hydrogen atoms is 6.628 Å. Because the van der Waals radius of the hydrogen atom is 1.20 Å, **MR** has a planar conjugate structure with a diameter of 4.228 Å.

*17. Energy-minimized structures of **MR** and X^{-1} (X = Cl, Br, and I) anion complexes simulated by Avogadro computer program*

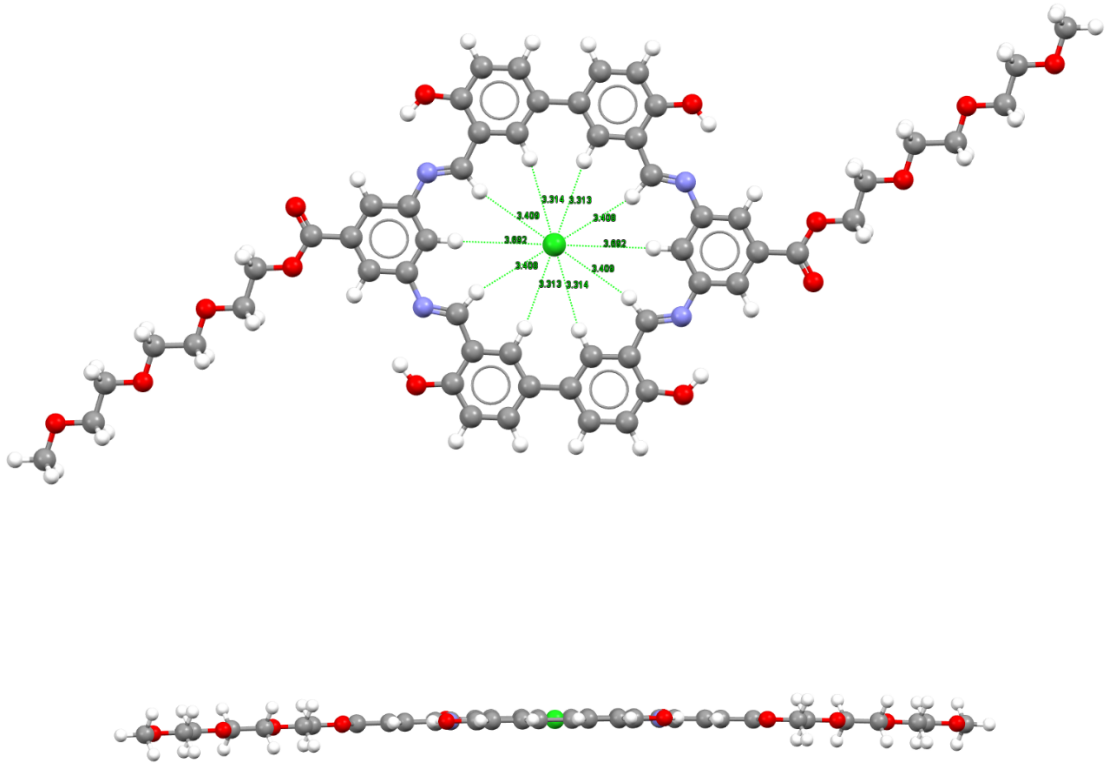

Fig. S34. Energy-minimized structure of **MR** and Cl^{-1} generated by Avogadro computer program.

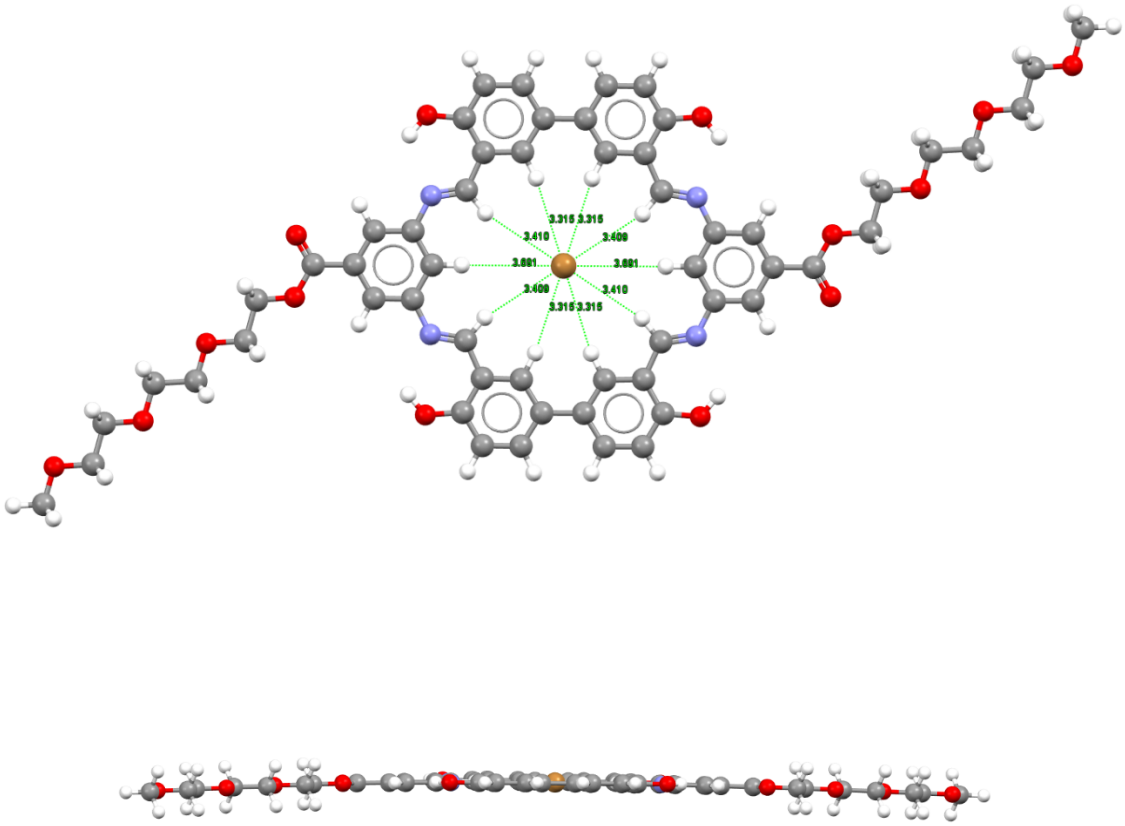

Fig. S35. Energy-minimized structure of **MR** and Br^{-1} generated by Avogadro computer program.

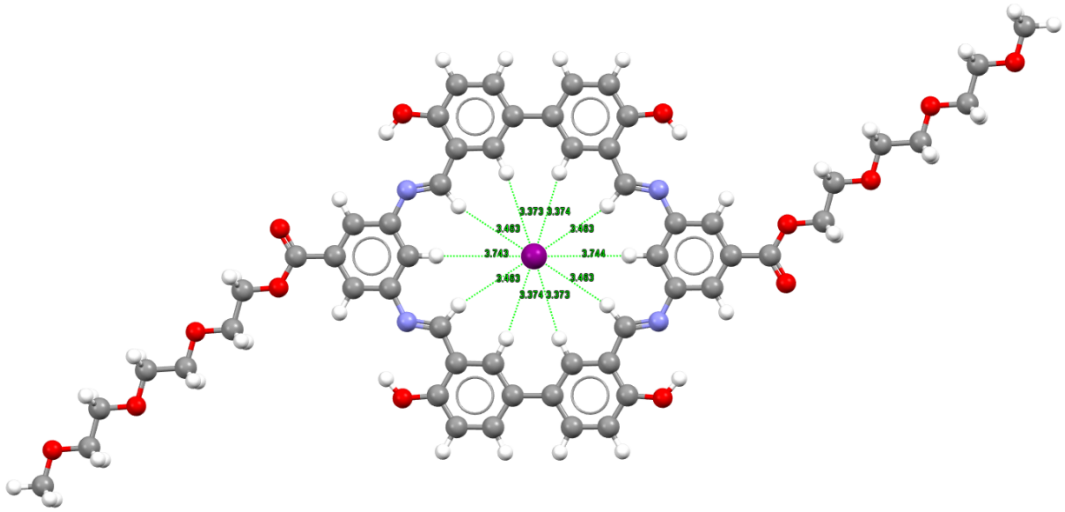

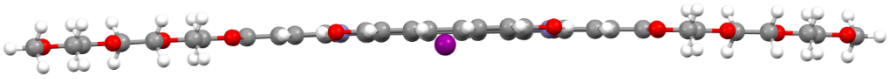

Fig. S36. Energy-minimized structure of **MR** and I^{-1} generated by Avogadro computer program.

References:

S1. W. Inoue, K. Kazama, M. Tsuboi and M. Miyasaka, *J. Photochem. Photobiol. A: Chem.*, 2022, **425**, 113688.

S2. E. Tzur, A. Ben-Asuly, C. E. Diesendruck, I. Goldberg and N. G. Lemcoff, *Angew. Chem., Int. Ed*., 2008, **47**, 6422-6425.

S3. Y. J. Lee, H. G. Heo and C. H. Oh, *Tetrahedron*, 2016, **72**, 6113-6117.

S4. S. D. Varakala, R. S. Reshma, R. Schnell and S. Dharmarajan, *Eur. J. Med. Chem.*, 2022, **228**, 113976.

S5. M. Li, K. Yamato, J. S. Ferguson and B. Gong, *J. Am. Chem. Soc.*, 2006, **128**, 12628-12629.

S6. K. J. Okolotowicz, P. Bushway, M. Lanier, C. Gilley, M. Mercola and J. R. Cashman, *Bioorg. Med. Chem.*, 2015, **23**, 5282-5292.

S7. A. N. Cammidge, R. J. Turner, R. D. Beskeni and T. Almutairi, *Liq. Cryst.*, 2017, **44**, 2018-2028.

S8. (*a*) T. Ackermann, *Ber. Bunsenges. Phys. Chem.*, 1987, **91**, 1398-1398; (*b*) P. R. Ashton, R. Ballardini, V. Balzani, M. Bělohradský, M. T. Gandolfi, D. Philp, L. Prodi, F. M. Raymo, M. V. Reddington, N. Spencer, J. F. Stoddart, M. Venturi and D. J. Williams, *J. Am. Chem. Soc.*, 1996, **118**, 4931-4951; (*c*) Y. Inoue, K. Yamamoto, T. Wada, S. Everitt, X.-M. Gao, Z.-J. Hou, L.-H. Tong, S.-K. Jiang and H.-M. Wu, *J. Chem. Soc. Perkin Trans. 2.*, 1998, 1807-1816.

S9. P. M. J. Job, *Ann. Chim. Paris.*, 1928, **9**, 113-203.